Final report dated 4 December 2023

WindSPORES

Policy-relevant wind power deployment scenarios for Switzerland

Source: Wallpaper Flare, public domain

Date: 4 December 2023

Location: Bern

Publisher:
Swiss Federal Office of Energy SFOE
Energy Research and Cleantech
CH-3003 Bern
www.bfe.admin.ch

Subsidy recipients:
ETH Zürich, Climate Policy Group
Universitätstrasse 16, 8092 Zürich
https://www.cp.ethz.ch/

Authors:
Francesco Lombardi, TU Delft, f.lombardi@tudelft.nl
Bryn Pickering, ETH Zürich, brynmor.pickering@usys.ethz.ch
Stefan Pfenninger, TU Delft, s.pfenninger@tudelft.nl

SFOE project coordinators:
Katja Maus, katja.maus@bfe.admin.ch
Lionel Perret, lionel.perret@bfe.admin.ch

SFOE contract number: SI/502229

Zusammenfassung

Der Ausbau der Windenergie könnte ein entscheidender, wenn auch wenig erforschter Bestandteil einer erfolgreichen Schweizer Energiewende sein. Unsere früheren Arbeiten – durchgeführt im Rahmen des WindVar-Projekts – haben gezeigt, dass eine erhöhte Windkraft für die Schweiz wirtschaftlich vorteilhaft sein kann, wenn sie eingesetzt wird, um von (anti)korrelierten Windmustern zwischen Schweizer Regionen sowie zwischen der Schweiz und ihren Nachbarn zu profitieren. Mit diesem Projekt bauen wir auf diesen Erkenntnissen auf, um zu zeigen, dass es in einer CO_2-neutralen Schweiz eine breite Palette kostengünstiger Optionen für den Einsatz von Windenergie gibt, darunter sowohl räumlich konzentrierte als auch verteilte Kapazitäten, und unterschiedliche Abhängigkeitsgrade an Windkraft für die Gesamtenergieversorgung. Dieser Optionsraum ermöglicht es Entscheidungsträgern, die Kompromisse zu verstehen, die ihre Präferenzen und Prioritäten mit sich bringen.

Um Windmuster in der Schweiz darzustellen, ist eine hohe räumliche und zeitliche Auflösung erforderlich. Wie im WindVar-Projekt identifizieren wir den regionalen Reanalysedatensatz COSMO-REA2 als die am besten geeignete Quelle für Windgeschwindigkeitsdaten. Damit sind wir in der Lage, bekannte meteorologische Phänomene abzubilden, die der kürzlich veröffentlichte Neue Europäische Windatlas (NEWA) nicht darstellen kann. Dies sind zum Beispiel Tagesschwankungen, die durch Berg-Tal-Brisen verursacht werden. Mit diesem Datensatz simulieren wir die Windenergieproduktion für verschiedene Turbinen-Archetypen, die auf kommerziellen Turbinen basieren. Wir wählen drei Archetypen mit besonders vorteilhaften Eigenschaften für den Einsatz in der Schweiz mit Nabenhöhen zwischen 120 und 160 Metern.

Wir integrieren unsere ausgewählten Windkraftanlagenmodelle in ein sektorengekoppeltes Modell des Schweizer Energiesystems und generieren auf Basis unseres SPORES-Algorithmus Hunderte von Möglichkeiten, wie Windenergie in ein CO_2-neutrales Schweizer Systemdesign passen könnte. Wir stellen fest dass verschiedene Turbinen-Archetypen in verschiedenen Regionen am besten geeignet sind, auch in Regionen wo die durchschnittlichen Kapazitätsfaktoren nicht ideal sind, das Platzieren von Windkapazität aber Vorteile für das Gesamtenergiesystem bringt, beispielsweise aufgrund einer besseren Korrelation mit regionalen oder gesamtschweizerischen Nachfragespitzen.

Einige Schweizer Regionen weisen die grössten Aussichten für den Ausbau der Windenergie auf, insbesondere die Jurakämme und die Hochebenen auf beiden Seiten der Jurakämme. Auch Gebiete innerhalb der Kantone Wallis, Graubünden, St.Gallen-Appenzell, und Ticino zeigen gewisses Potential, mit Unterschieden zwischen Turbinentypen. Darüber hinaus zeigen wir, dass der gleichzeitige Einsatz von Turbinen in Regionen mit besonders antikorrelierten Windmustern zu komplementären Erzeugungsmustern und einem insgesamt stabileren systemweiten Erzeugungsprofil führen könnte. Insbesondere favorisiert unser Modell den Zubau von Wind in den Alpenkantonen Wallis und Uri zusammen mit dem Zubau im Kanton Solothurn. Systeme mit hohem Windenergieeinsatz, die von diesen synergistischen Zubaustrategien profitieren, sind

auch robuster gegenüber unsicheren Wetterjahren und Änderungen der Systemdesignentscheidungen in Nachbarländern.

Insgesamt zeigen unsere Ergebnisse, dass es ein grosses technisch-ökonomisches Potenzial für die Windenergie als Teil eines zukünftigen Schweizer Energiesystems gibt. Im Vergleich zur Solarenergie weisen Systemdesigns, die stärker auf Windenergie basieren, zusätzliche technische Vorteile auf, wie z. B. einen geringeren Bedarf an Speicher- und Elektrolysekapazität und eine höhere Robustheit gegenüber der Unsicherheit der Randbedingungen. Da Solarenergie in der Regel auf eine höhere gesellschaftliche Akzeptanz stösst (zumindest bei Einsatz in der gebauten Umgebung), müssen Entscheidungen über Turbinengrösse und -platzierung sorgfältig getroffen werden, um sicherzustellen, dass die Vorteile der Windkraft genutzt werden können.

Summary

The expansion of wind power may be a critical, although underexplored, component of a successful Swiss energy transition. Our previous work – undertaken in the WindVar project – showed that increased wind power can be economically favourable to Switzerland, if deployed to capitalise on (anti)correlated wind patterns between Swiss regions and between Switzerland and its neighbours. With this project, we build on this finding to show that there exists a wide range of cost-effective wind power deployment options in a carbon-neutral Switzerland, including spatially concentrated and distributed capacity and varying levels of reliance on wind for energy supply. This option space enables decision makers to understand the trade-offs entailed by their preferences and priorities.

A high spatial and temporal resolution is required to depict wind patterns in Switzerland. As in the WindVar project, we identify the COSMO-REA2 regional reanalysis dataset as the most suitable source of wind speed data. With it, we are able to depict known meteorological phenomena that the recently published New European Wind Atlas (NEWA) cannot; for example, diurnal variability caused by mountain-valley breezes. With this dataset, we simulate wind power production for many turbine archetypes based on commercially available turbine models, and select three archetypes with particularly promising features for Swiss wind patterns, with hub heights ranging from 120 to 160 metres. We integrate our chosen wind turbine archetypes in a sector-coupled model of the Swiss energy system and, based on our SPORES algorithm, generate hundreds of ways in which wind power could fit into a carbon-neutral Swiss system design. We find that different archetypes perform best in different areas, including in areas where their capacity factory is less-than-ideal but benefits for the system are high, for instance, due to a better correlation with regional or overall Swiss demand peaks.

Some Swiss regions show the most promise for wind power deployment. In particular, the Jura crests, and the plateaus on either side of the Jura crests. Some promise is also shown by areas within the cantons Valais, Graubünden St.Gallen-Appenzell and Ticino, with differences across turbine models. Furthermore, we reveal that deploying turbines simultaneously in regions with particularly anti-

correlated wind patterns might lead to complementary generation patterns and to an overall more stable system-wide generation profile. In particular, deployment in the Alpine cantons of Valais and Uri correlates with deployment in the canton of Solothurn north of the Alps. Systems with high wind power deployment that capitalise on these synergistic patterns and complement them with diverse hotspots in other promising regions also perform more robustly against uncertain weather years and changes in system design choices in neighbouring countries.

Overall, our findings show that there is a large techno-economic potential for wind power to be part of a future Swiss energy system. Compared to photovoltaics, system designs relying more on wind power show additional technical benefits, such as a reduced need for storage and electrolysis capacity and higher robustness against the uncertainty of boundary conditions. As photovoltaic power is typically met with higher social acceptance (at least when deployed in the built environment), decisions on turbine size and placement need to be carefully navigated to ensure the benefits of wind power can be realised.

Main findings

- COSMO-REA2 is confirmed as the most suitable regional meteorological reanalysis dataset for analysing Swiss wind patterns.
- In line with the expectations, the most interesting turbines for Switzerland are recent models with 120 to 160 m hub heights.
- There are hundreds of feasible and cost-effective configurations for wind power in Switzerland
- The Jura crests and the plateaus on both sides of them are the most promising siting areas.
- Deployment making use of synergistic weather patterns along the North-South axis benefits system balancing.
- A substantial, synergistic deployment aids the robustness of the wider energy system, reducing the need for energy storage and electrolysis capacity.

Contents

1 Introduction

1.1 Background information and current situation

The Swiss Energy Strategy 2050 aims to progressively phase out nuclear and fossil-fuel power plants. Considering the modest potential for further expansion of hydropower capacity, this will require an increasing deployment of solar and wind power. However, the expansion of wind power remains an underexplored component of a successful Swiss energy transition. We have previously shown that, under typical weather conditions, there is maximum economic value for Swiss wind power in specific locations (Jura crests, Alpine crests, Lake Geneva region), some of which also take advantage of anti-correlation with typical wind generation patterns in neighbouring countries [1]. Nevertheless, wind power deployment at such locations might not necessarily encounter the highest social support nor be most resilient to the uncertainty of complementary system design choices within Switzerland and neighbouring countries. Different wind power deployment options may exist that can deliver close-to-maximum economic value in a future where a large fraction of electricity comes from variable renewables. These options could benefit from having higher social acceptability, providing grid stability under average weather conditions, and resilience against unusually adverse weather conditions compared to typically favoured siting locations. Quantifying the trade-offs between these different aspects, rather than optimising for only one of them, can better support wind power deployment choices and lead to more socially and politically viable system design decisions.

1.2 Purpose of the project

To explore possible configurations of wind power within a future Swiss energy system, three modelling components are necessary: a high-resolution understanding of wind power potential, a high-resolution representation of a Swiss energy system encompassing all energy demands, and the ability to generate an option space of solutions, not just one or a handful of economically optimal ones. In this project, we design each of these three components and apply them to exploring wind power deployment options for Switzerland.

1.3 Objectives

In particular, we investigate the following research questions:

1. **Which wind turbine models are most promising for Swiss wind patterns?** We consider seven model archetypes at different hub heights, leading to seventeen different possible combinations of turbine and hub height. Based on the analysis of their performance across seven weather years, we select three model archetypes, with hub heights ranging from 120 to 160 m, for further analysis.

2. **What is the design space for wind power deployment in a carbon-neutral Switzerland?** We generate hundreds of ways in which wind power could fit into a carbon-neutral Swiss energy system configuration. Hence, we look at the most frequent design choices, in terms of turbine archetype and location, in the generated option space, and at synergies across deployment sites. Some regions stand out as particularly attractive, but there are differences across turbine archetypes. We also look at correlations between wind power and other pieces of energy infrastructure and show how wind could limit the need for battery storage and electrolysis capacity.

3. **How robust are alternative wind power configurations with respect to the uncertainty of weather regimes and neighbouring countries' design choices?** We select six representative wind power deployment options from the generated design space, which differ in terms of geographical distribution and the total amount of wind power capacity, and we test their operation across sixteen boundary conditions. We see that capitalising on a diverse mix and spatial distribution of turbines ensures more robust results. Some of the synergies identified in the previous stages of analysis are confirmed to be particularly attractive.

2 Methods

We first discuss how to achieve a high-resolution representation of Swiss wind patterns and corresponding turbine capacity factors (sub-section 2.1). We then present the adopted energy system model (sub-section 2.2) and the modelling workflow to generate hundreds of alternative near-optimal wind deployment and energy system design options (sub-section 2.3).

2.1 Simulating Swiss wind patterns and turbine outputs

2.1.1 COSMO-REA2 and NEWA meteorological datasets

To model renewable generation profiles in energy systems, we often rely on a crucial tool: meteorological reanalysis. Meteorological reanalysis is a method to combine historical weather measurements with state-of-the-art weather forecast models to generate consistent, historical time series of weather conditions, either globally (global reanalysis) or regionally (regional reanalysis). Most studies on renewable energy in Europe, including our own prior work [2, 3, 4, 5], are based on global meteorological reanalyses. The quasi-standard dataset often used is MERRA-2, with a 55 km horizontal resolution [6], slowly being replaced by ERA-5, which has a similar spatial resolution as MERRA-2. This spatial resolution is too coarse for Switzerland. Indeed, anything coarser than a 2-3km resolution risks overlooking the meteorological phenomena that could make wind power a viable component of a future Swiss energy system [7, 1].

In our previous work, we focussed on two versions of the COSMO reanalyses operated by the German Weather Service DWD: COSMO-REA6, at 6km resolution covering all of Europe, and COSMO-REA2, at 2km resolution, covering only Germany and neighbouring countries, which includes Switzerland [8]. Here, we continue using COSMO-REA2, since we found that it is capable of reproducing some of the wind phenomena at measurement sites across the country, for example, diurnal variability caused by mountain-valley breezes, and the Föhn and Bise channelling flows. However, we also analyse the relative performance of the recently developed New European Wind Atlas (NEWA), which provides hourly data at a 3km resolution across all of Europe [9, 10]. A possible advantage of NEWA is its temporal scope: it spans more years than COSMO-REA2.

COSMO-REA2 has a high spatial resolution of around 2km. Nonetheless, the COSMO reanalysis products have been shown to only represent wind phenomena at six to eight times coarser spatial resolutions (i.e. their 'effective resolution') [11]. Therefore, we would expect wind systems of a scale of 14km to be resolved with COSMO-REA2. In Switzerland, this is sufficient to represent the channelling in the Swiss Plateau region between the alpine and Jura ranges, Föhn flows in major alpine valley outlets and mountain-valley breezes in the broad Rhone valley [1].

NEWA is based on a dynamical downscaling of ERA5 using the Weather Research and Forecasting (WRF) model evaluated against mast measurements and exists as a mesoscale and microscale product for the European continent [9, 10]. The spatial resolution of the mesoscale NEWA is 3 km at seven heights above ground level and provides wind speed and power density over the period 1989 to 2018. The NEWA microscale atlas is based on a second linearized downscaling to 50 m spatial resolution and has been found to improve long-term means when compared to observations [9]. However, in practice, only the mesoscale data is available for public download, and only for the period 2009 to 2018 at an hourly resolution. An overview of the two datasets is given in Table 1. In the following sections, we will refer to both wind speeds and wind turbine capacity factors.

	Spatial Extent	Resolution	Temporal Extent	Resolution
COSMO-REA2	AT, BE, DK, DE, LI, LU, NL, SI, CH	2 km	7 years (2007 - 2013)	1 h
NEWA	Europe excl. IS, incl. TR	3 km	10 years accessible (2009 - 2018)	1 h

Table 1: Key characteristics of COMSO-REA2 and NEWA datasets.

2.1.2 Extrapolating wind speeds and wind turbine capacity factors

We take fixed-height wind speeds from both datasets directly. Using a log-law regression, we derive coefficients of the wind speed vertical profile in each grid-cell and hour, which we can then use to simulate wind speeds at any height, e.g., to match a specific wind turbine hub height. We simulate wind turbine capacity factors using these wind speeds and the performance curves of specific wind

turbines. We cannot use the underlying method of the Virtual Wind Farm (VWF) model described in the study by Staffell and Pfenninger [6], for two reasons. First, the VWF model uses smoothed wind turbine performance curves which represent the aggregate performance of an entire wind park. However, Switzerland's orography and land use patterns mean that wind parks in the country are small, sometimes constituting only a single turbine. Second, Switzerland was not included in the bias correction process. This means that bias correction factors will be predominantly affected by large wind parks in flat terrain. We do not believe that such a bias correction would be fruitful for our analysis. Attempting to bias correct using data in Switzerland would be equally fruitless with the available data, since correlation distances (the distance over which weather data in one location reliably correlates with weather data in another) are short, due to the country's complex orography. Therefore, we use single wind turbine performance curves and do not attempt to bias-correct. In the remainder of this section, simulated wind speeds are those derived from the log-law regression, and simulated capacity factors are those derived from interpolating simulated wind speeds along wind turbine performance curves.

Wind turbines are designed in such a way that different ones will perform best under particular wind conditions. Some turbines perform quite poorly at low wind speeds (high 'cut-in'speeds), but reach their maximum performance ('rated output') very quickly, potentially providing more consistent capacity factors throughout the year. Others have a lower cut-in speed, but also only reach their rated output at higher wind speeds. Finally, wind turbines are designed to operate at specific heights above the ground (hub height). Although this is not usually a component considered in energy system models, we include turbines designed for different hub heights in this analysis, since one trade-off that might exist in Switzerland is to accept lower turbine performance by limiting the hub height. Therefore, we consider seven turbine archetypes based on models that are currently deployed in Europe. All the turbine models our archetypes are based on are sold for installation within specific hub height ranges, as shown in Table 2. By taking six fixed hub heights – 60, 80, 100, 120, 140 and 160m – we represent seventeen different possible combinations of turbine and hub height. We will discuss these seventeen combinations and select four for subsequent analysis and inclusion in the energy system model.

Once the dataset and wind turbines are selected, one must aggregate the capacity factor profiles described across Switzerland's tens of thousands gridcells into a tractable number of regions for the energy system model. The approach adopted for clustering spatial regions is laid out in Appendix 8.

2.2 Energy system model and generation of alternative near-optimal system designs

We build on our Sector Coupled Euro-Calliope model (SC-EC) to represent the Swiss and European energy systems at a high spatial and temporal resolution [13]. SC-EC takes the current configuration of all European energy consumption as a departure point to model credible future configurations in a realistic manner.

Turbine archetype	Based on model	Hub height range (m)	Nominal capacity (kW)	Projected cost (EUR/kW)*	Rationale	Considered in system study
Medium-size established model A 80m	Vestas V112	69 - 94	3450	1697	Previously deployed in Switzerland	no
Medium-size established model B 60m	Enercon E82	59 - 84	3000	1697	Previously deployed in Switzerland	no
Medium-size established model C 120m	Vestas V110	80 -125	2000	1697	Widely deployed in Europe	no
Small established model 60m	Enercon E53	60 -75	800	1697	Widely deployed in Europe	no
Medium-size recent model 120m	Enercon E92	78 - 138	2350	1697	Recent model considered promising for Switzerland	**yes**
Large-size recent model A 160m	Enercon E138	81 - 160	4200	1697	Recent model considered promising for Switzerland	**yes**
Large-size recent model B 160m	Enercon E160	120 - 166	5500	1697	Recent model considered promising for Switzerland	**yes**

Table 2: Electricity generation, hub height range and cost of studied turbine archetypes, including the commercial model they are based on, the rationale for their selection and anticipation of whether they are used in the system study. Technical data was retrieved from the manufacturers' datasheets. The hub height is given as vertical height above ground. *Projected costs are based on the average 2050 costs from a recent Swiss-specific study [12], converted to EUR.

Compared to the single energy carrier considered in power system models, we represent 13 carriers in SC-EC: electricity, hydrogen, CO_2, liquid and gaseous hydrocarbons (kerosene, methanol, diesel, and methane), solids (residual biofuel and municipal waste), low-temperature heat (combined space heat and hot water, and cooking heat), and vehicle distance (heavy- and light-duty road vehicles). These carriers can be consumed, produced, and converted by a variety of technologies to meet demand. In addition, low-temperature heat, hydrogen, electricity, and methane can be stored. Since future international energy commodity prices are highly uncertain, energy imports from outside our model region are not allowed. Accordingly, all our model results represent system designs in an energy-self-sufficient Europe. The full representation of carrier and technology connections is given in Figure 1. Further detail is given in the Experimental Procedures of Pickering *et al.* [13].

To represent Swiss wind power generation at a high spatiotemporal resolution, we have made modifications to the base SC-EC, which we explain here.

First, we update the approach and thresholds to calculate the land area available for wind power generation. The data processing workflow, detailed in [14], uses gridded elevation and land-use data to limit the land which is technically available for deployment. We improve the initial processing workflow by increasing the spatial resolution of elevation data, to the 25m EU-DEM v1.0[1], and changing thresholds associated with existing land use. We allow land-use gridcells with up

[1] https://land.copernicus.eu/imagery-in-situ/eu-dem/eu-dem-v1-0-and-derived-products/slope

to 10% building share to be eligible for wind power deployment, up from 1%. We also allow gridcells with up to 33% urban green share to be eligible, up from 1%. These threshold increases reflect the reality in Switzerland as they ensure all existing wind turbine sites are in eligible land-use gridcells. The final area available for wind power deployment is 47% of total Swiss land area, up from 16.5%. This increase is mostly caused by the use of higher resolution elevation data, which enables slope data to be more accurately inferred and, therefore, more valleys and mountain plains to be included. Assuming a wind turbine deployment density of 8 MW/m^2 [15], our updated analysis leads to space for 51,643 3MW turbines. This is similar to the potential for 50,400 3MW turbines calculated independently by Dujardin *et al.* [16], which they deem to be a conservative estimate. Figure 2 outlines the geographical distribution of the deployment potential for wind generation capacity.

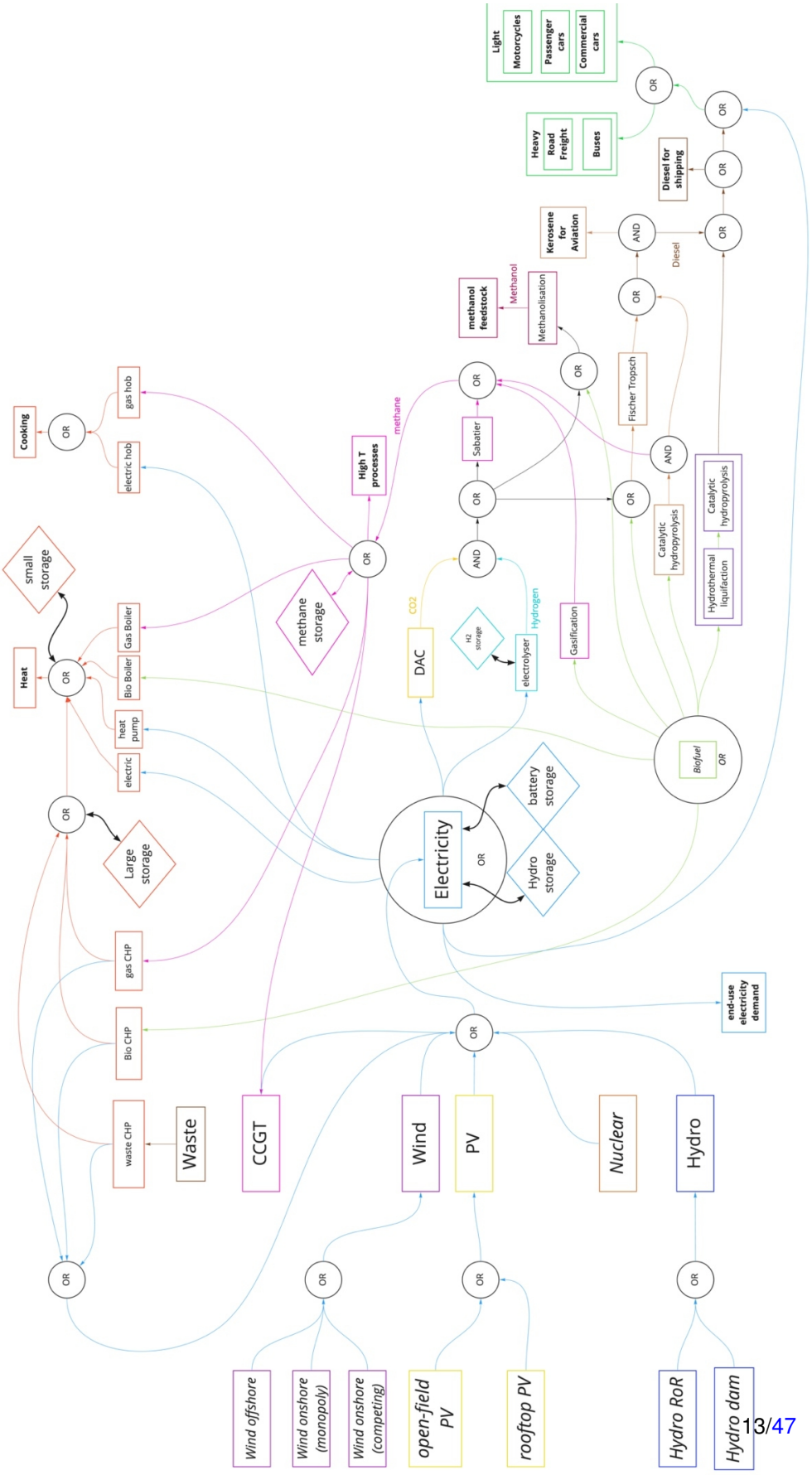

Figure 1: Flow chart of the Sector-Coupled Euro-Calliope model, including supply technologies, energy carriers, and demand sources. AND and OR icons in the flow indicate when an in/output is a combination (AND) or choice (OR) of out/input. Where energy enters the systems from an external resource, the carrier is given in italics (e.g. Waste). Storage technologies are depicted as diamonds. Bold text refers to demands, where energy exits the system. Flow line colours are related to the energy carrier flowing along that line.

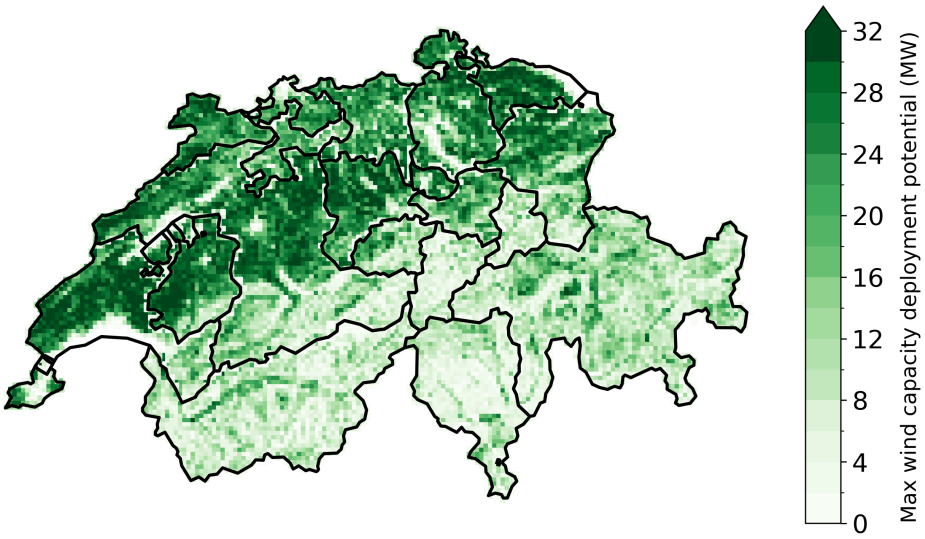

Figure 2: Maximum spatial potential for wind generation capacity deployment across every gridcell. Gridcells are then aggregated into the 65 turbine-specific clusters identified in sub-section 3.3 based on each turbine's capacity factors, thereby providing a cluster-aggregated maximum potential for wind capacity deployment as an input to the energy system model.

Second, we increase the resolution of model regions in Switzerland, from two to twenty. This increased resolution enables us to better resolve the diversity of building and industry demands and the capacity factor profiles of PV and hydropower. Furthermore, we better represent transmission bottlenecks with these regions. Inter-regional grid transfer capacities have been estimated as part of the NEXUS-E modelling platform development[2] using the network topology according to Swissgrid. These capacities act as a lower bound in our model, with the option to pay to increase them. This grid topology also dictates the composition of our model regions. The regions are based on cantonal boundaries, with some smaller or surrounded cantons merged into neighbours. Table 3 shows the mapping from canton to model region number. To handle this higher spatial resolution in Switzerland (including 195 wind power profiles, see below), we reduce the resolution of other areas in Europe to the national level. The final 54 model regions (34 European countries and 20 Swiss sub-regions) are shown in Figure 3.

Third, as detailed in Appendix 8, we represent wind power options in Switzerland using three wind turbine archetypes across 65 clustered spatial areas. Therefore, we have 195 hourly wind turbine capacity factor profiles in Switzerland. In most model regions, there are several clusters. We do not model the grid connection requirements of these clusters within model regions; wind turbine generation across clusters in a region contributes to the total regional wind power without any cost or losses for intra-regional transmission. Only inter-regional transmission

[2] https://nexus-e.org/

is considered.

Canton	Model region number	Canton	Model region number
Vaud	1	Glarus	11
Valais	2	Appenzell Ausserrhoden	12
Geneva	3	Appenzell Innerrhoden	12
Bern	4	St. Gallen	12
Fribourg	5	Graubünden	13
Solothurn	6	Thurgau	14
Neuchâtel	4	Luzern	15
Jura	7	Uri	16
Basel-Stadt	8	Schwyz	17
Basel-Landschaft	8	Obwalden	18
Aargau	9	Nidwalden	18
Zürich	10	Zug	19
Schaffhausen	10	Ticino	20

Table 3: Mapping from 26 Swiss cantons to 20 Euro-Calliope model regions.

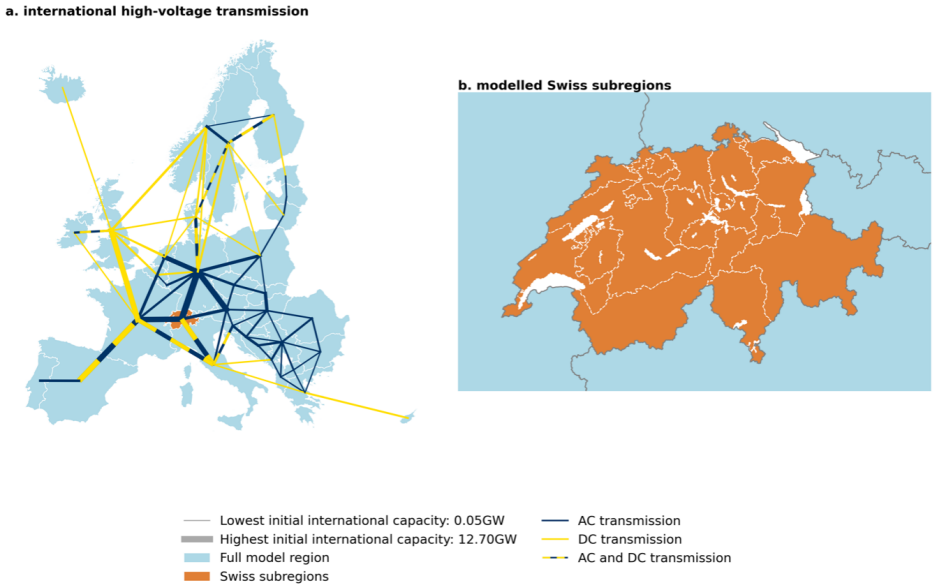

Figure 3: Sector-Coupled Euro-Calliope model regions, modified for the Wind-SPORES project. **a.** all international model regions, including the high-voltage transmission grid topology. Lines are coloured based on the type of transmission available between countries. Thicker transmission lines represent larger modelled initial grid transfer capacities. All lines can expand beyond their initial capacities. **b.** Focus on the 20 subregions in Switzerland. White spaces depict large water bodies. For clarity, the transmission network is not shown within Switzerland, only the region borders.

Fourth, we update our cost assumptions for key energy supply technologies based on the Switerzland-specific analysis by Bauer *et al.* [12]. Those include: wind, roof-mounted solar photovoltaic, and open-field solar photovoltaic. We do not update costs of other techologies, such as batteries and electrolysers, since the analysis by Bauer *et al.* [12] for those technologies does not include considerations specific to Switzerland. Thus, we deem it more sensible to ensure homogeneity with the cost source we use for every other technology not analysed by the above study. Cost assumptions for such other technologies are the same used in Pickering *et al.* [13], and mostly derived from the Danish Energy Agency technology catalogue. Finally, we set up an ad-hoc workflow for our SPORES algorithm [3, 17] for the generation of equally feasible design options. Based on the latest findings from other ongoing projects, we anticipate that the generation of a large number of near-cost-optimal alternatives is most likely to immediately include the qualitative storylines (e.g., 'High Wind dependence'), without the need to model them separately. Instead, parametric scenarios (such as changes in weather conditions or rest-of-Europe system design) need to be taken into account explicitly. We have modified our workflow for the generation of feasible solutions accordingly, as further detailed in the following sub-section.

2.3 Sets of design options and uncertainty scenarios

Based on our updated model setup and our 'Baseline' set of boundary conditions for Switzerland (reflecting the Swiss Energy Perspectives 2050+ ZERO basis scenario, as further detailed in Appendix 9), we devise an original modelling approach that allows us to tackle both the limitations of conventional cost optimisation and the uncertainty associated with model parameters. The approach is depicted in Figure 4, and foresees two stages of analysis: i) the generation of alternative feasible wind power and energy system designs for Switzerland, via SPORES, based on different willingness to pay and weather conditions; and ii) the out-of-sample testing of the performance of representative Swiss energy system configurations against a broader range of uncertain parameters (additional weather years, design choices in neighbouring countries).

More precisely, we use our SPORES algorithm to generate hundreds of feasible system designs for the Swiss energy system, initially investigated as an isolated system. All these feasible Swiss energy system designs are economically comparable, within 5-to-10% of the minimum feasible system cost for a given weather year, but different in terms of which technologies they deploy and where. We use the latest version of the SPORES algorithm, presented in detail in Lombardi *et al.* [17]. We consider two weather years, identified as 'typical' (2012) and 'adverse' (2010), among those available both in the SC-EC dataset and in COSMO-REA2. The SPORES-generated option space naturally includes system designs that match the features of possible qualitative storylines. Therefore, there is no need to model them separately. By looking at the frequency of wind turbine deployment across regions in the resulting broad option space (which includes up to 484 different options), and at correlations across deployment sites to discover possible synergies therein, we identify the most promising deployment sites and turbines. Furthermore, we complement this by examining the correlation between total wind capacity and other pieces of infrastructure for a carbon-neutral Swiss system, thereby providing an initial picture of how and where wind deployment could impact the Swiss energy transition.

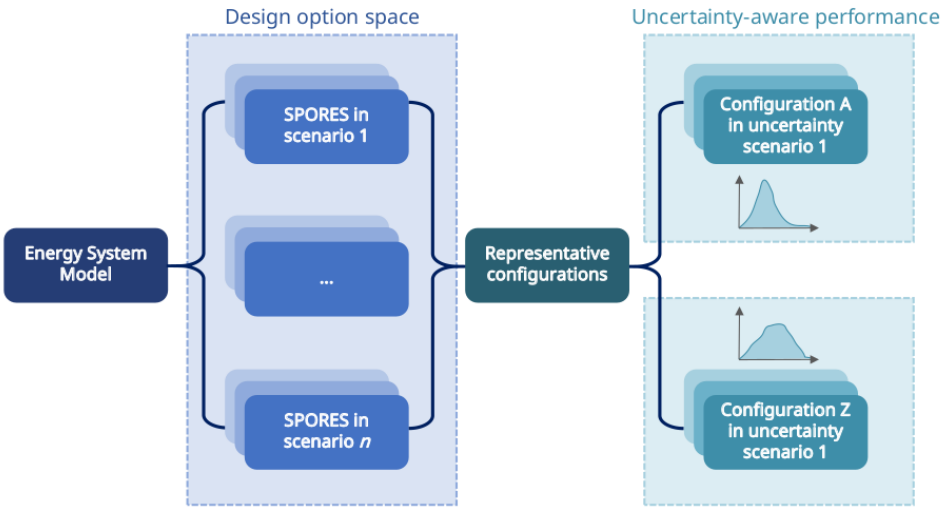

Figure 4: Flow chart summarising the original modelling approach designed for this project. First, near-optimal energy system design options are generated via our SPORES algorithm for different cost relaxations and weather years (see Table 4). Hence, representative configurations are selected for a second-stage analysis in which their operation is tested 'out-of-sample' against a variety of uncertain conditions, including more weather years and different system designs in neighbouring countries. This allows comparing the performance of two alternatives, for any metric of interest, by means of probability density functions that account for the uncertain nature of future operating conditions.

From the most promising options, we select representative system designs for further analysis. We choose the designs so that they cover increasing percentiles of total wind capacity deployment, while also being different from each other in the way they deploy wind generation capacity in Switzerland (informed by the first-stage analysis above), thereby synthesising the depth and breadth of the option space for wind deployment in the country. These representative system designs allow further investigation of the uncertainty concerning deviations in the assumed boundary conditions, now also including the behaviour of neighbouring European countries.

In fact, we test the performance of the selected representative system designs across various plausible 'out-of-sample' (i.e., off-design) conditions (Table 4, 'Scenarios for out-of-sample testing'). Those shall include all four weather years (2010-2013) that exist both in COSMO-REA2 and in the SC-EC database, in such a way as to check the impact of weather regimes on the system performance. In addition, we test the impact of other European countries behaving in different ways, picking up four radically different European energy system designs from a set of equally viable options, generated via SPORES in a separate, dedicated run. As a result of the out-of-sample testing of the identified representative design options, we communicate their performance in a 'probabilistic' manner, which accounts for the uncertainty of future boundary conditions. For instance, in terms of costs, import-export balance or grid-stability benefits, a given system design

will not be strictly better or worse than another but rather more or less likely to perform better, depending on how the rest of Europe behaves and on the weather regimes. This also ensures that the assumptions associated with the Swiss EP 2050+ ZERO basis scenario in terms of European energy prices are not problematic since the identified configurations are tested for various European energy system conditions.

Scenarios for generating alternatives	Resulting design options
Swiss EP 2050+ ZERO basis, typical weather (+5% willingness to pay)	121
Swiss EP 2050+ ZERO basis, critical weather (+5% willingness to pay)	121
Swiss EP 2050+ ZERO basis, typical weather (+10% willingness to pay)	121
Swiss EP 2050+ ZERO basis, critical weather (+10% willingness to pay)	121
Scenarios for out-of-sample testing	**Resulting boundary conditions**
Weather years 2010-2013	4
Rest-of-Europe alternative system design	4 per weather year

Table 4: Summary of high-level scenarios employed in this project in the two stages of i) generating alternatives and ii) testing the most representative options in out-of-sample conditions. All Swiss scenario variants build on our imitation of the EP 2050+ ZERO basis scenario, which we do not replicate exactly (see Appendix 9). We generate near-optimal design options within the boundary conditions defined by this scenario for two levels of 'willingness to pay more' (5% and 10%) compared to the least-cost feasible solution, which we replicate for both typical and critical weather. Finally, we use 4 weather years and 4 radically different feasible designs for the rest of Europe per weather year (leading to a total of 16 possible combinations) to test out-of-sample the most representative Swiss system designs.

It is worth noting that the adopted model setup, with decisions on 65 sub-national wind deployment areas for each turbine within Switzerland to be paired with whole-country decisions for neighbouring countries, is extreme in terms of solving complexity and may be prone to numerical trouble, namely difficulty for the solver to find a solution due to the sheer size of the problem. Whenever numerical trouble arises, we accept marginal relaxations of the selected system configuration to facilitate the solver. In practice, this might mean that some configurations can adapt with small additional (dis)investments to cope with adverse conditions. To check for this behaviour, we will also examine investment costs as part of our performance comparison, expecting these to vary only marginally across the out-of-sample optimisations.

3 Results and discussion

3.1 Wind power potential and turbine performance

3.1.1 COSMO-REA2 is the most suitable dataset for analysing Swiss wind alongside other wind patterns in Europe

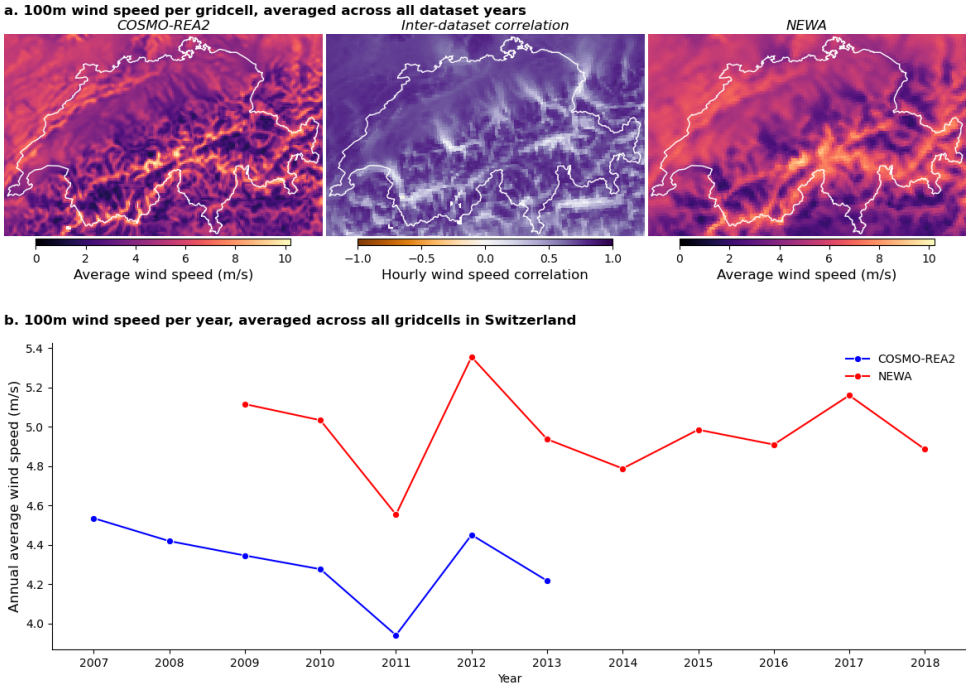

Figure 5: Comparison of simulated wind speeds from NEWA and COSMO-REA2 datasets. **a.** average annual wind speed per grid-cell (left and right) and Pearson correlation between hourly wind speeds of the two datasets in each gridcell (centre). Inter-dataset correlation is undertaken after spatially resampling COSMO-REA2 data to match the gridcell size and position of the more coarse NEWA data. **b.** Annual average wind speeds for all gridcells in Switzerland for the two datasets. The two datasets span different spatial scopes: 2007 – 2013 (COSMO-REA2) and 2009 – 2018 (NEWA), leading to five years of overlapping data.

Figure 5 shows wind speeds at 100 m, averaged spatially and temporally. Both datasets resolve the impact of Swiss orography on wind speeds, with highest average speeds on alpine peaks and along the upper Rhone and Rhine valleys (Figure 5a). However, the smoothing effect of NEWA's coarser resolution is also apparent. Although there are no locations in Switzerland where the two datasets fundamentally contradict each other - i.e., there are no anticorrelated timeseries in any location - NEWA does not perform as well as COSMO-REA2 in representing valley flows. The central panel in Figure 5a highlights the lack of correlation between the two datasets in all valleys and valley outlets, which is driven by the inability of NEWA to capture the summertime mid-afternoon increase in wind

speeds experienced in the valleys. We can verify this by focussing on a specific site where we know this phenomenon exists. Figure 6a shows the measured performance of a wind turbine in Martigny, situated in the Rhone valley. In the summer mid-afternoon, wind speeds (and, accordingly, capacity factors) consistently reach their highest levels at this site. This is well captured by COSMO-REA2, but not by NEWA, which has a 4x lower mid-afternoon peak. We can verify that it is not strictly the spatial resolution creating this disparity, since COSMO-REA2 maintains a strong increase in turbine capacity factor even after regridding the data to match NEWA. The performance of NEWA at Martigny is slightly better than we previously found for COSMO-REA6 and MERRA-2 [1], but is generally closer in performance to those coarser datasets than it is to COSMO-REA2 or measured data.

Although it does not capture the strength of summer valley flows, NEWA depicts a higher average annual Swiss wind speed than COSMO-REA2 (Figure 5b). In five overlapping years between the two datasets, we can see the same general pattern: 2011 was a particularly poor year, while 2012 was conversely a particularly strong one. We cannot know which of these two datasets best represents actual average annual wind speeds, but it is likely that NEWA is overpredicting productivity in some regions and times of the day. Figure 6b shows the case of St. Brais, a wind park along a ridge in the Jura mountain range. In winter, both datasets overpredict wind turbine productivity, up to 2.5x and 5x for COSMO-REA2 and NEWA, respectively. NEWA also severely overpredicts in summer at St. Brais, particularly overnight.

Yet, it is not straightforward to definitively claim that COSMO-REA2 is the best dataset for representing meteorological phenomena in Switzerland. Indeed, in winter at Martigny (Figure 6a), NEWA captures the slight increase in turbine capacity factor in the mid-afternoon. This is missed entirely by COSMO-REA2, which instead shows the capacity factor peaking in the morning, followed by a steady decline until early evening. However, for our particular use case, COSMO-REA2 does seem to be the most preferable option. We wish to explore the contribution of Swiss wind power to a future energy system which relies predominantly on variable renewable generation. Since average wind capacity factors in Switzerland are low compared to neighbouring countries, it is prudent to capture those instances where the inverse is true, i.e., summer afternoons, when Swiss wind capacity factors reach their peak. Therefore, we continue our analysis using COSMO-REA2 data only.

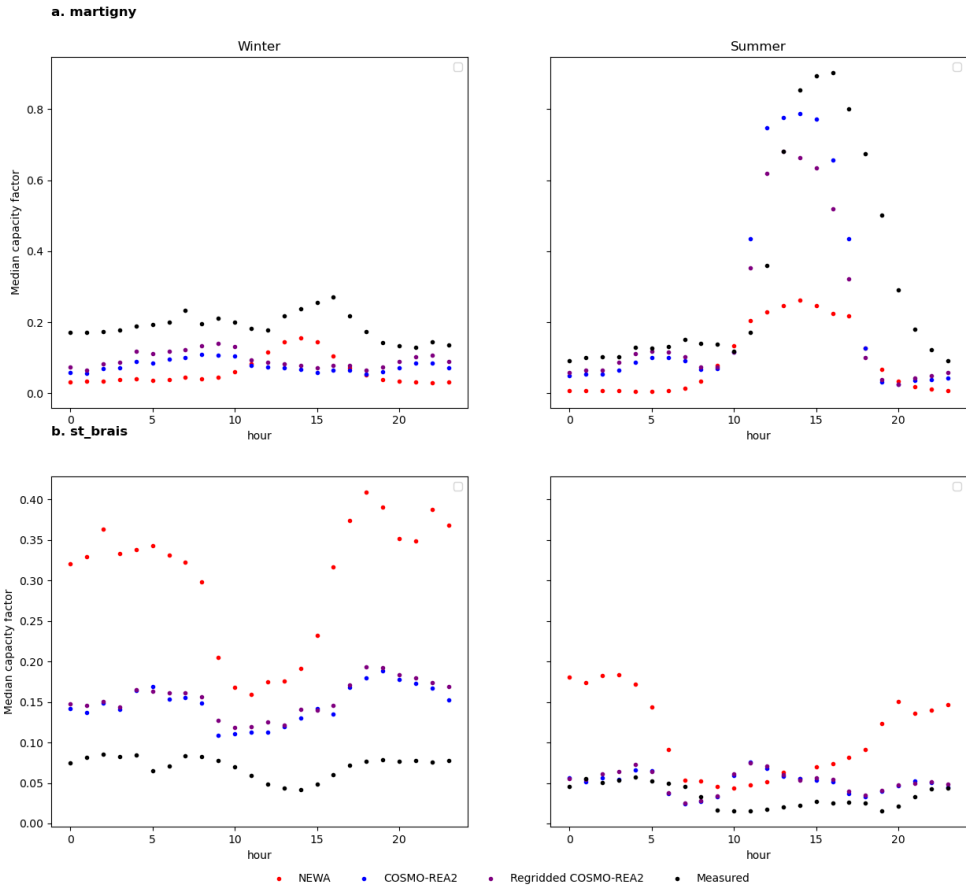

Figure 6: Comparison of simulated and measured wind turbine median hourly capacity factor at two wind turbine sites in Switzerland. **a.** The Martigny site is in the Rhone valley "knee", as the valley changes direction in the south-west of canton Valais. **b.** The St. Brais site is in the Jura mountain range. Gridded NEWA/COSMO-REA2 data has been interpolated to geographic coordinates of turbines sites. Median capacity factors are taken for each hour of the day, for all days in winter (Dec-Feb, left) and summer (Jun-Aug, right) in the years 2012 – 2013 (where data overlap exists for all datasets). "Regridded COSMO-REA2" refers to the COSMO-REA2 data (approximately 2km horizontal resolution) spatially resampled to the same gridcell size and position as NEWA data (approximately 3km horizontal resolution).

3.1.2 Turbine archetypes based on recent commercial models show more promise than those based on established models for further analysis

Figure 7 compares all the considered turbines. The power curves of the *Medium-size recent model*, *Large-size recent model A* and *Large-size recent model B* suggested by SFOE are relatively similar (Figure 7a) to the power curve of the *Small established model*, whilst they are slightly different from those of the *Medium-size established models A* and *C* and markedly so from the power curve of the *Medium-size established model B*. What is more, despite the similarity of the

SFOE-suggested recent models to the *Small established model* in terms of power curves, the capacity factor duration curve for average Swiss wind conditions (Figure 7b), which gives the hourly values ordered from highest to lowest values, shows substantial differences. This results from the different turbine sizes, with some of the recent models reaching even more than double the hub height of the *Small established model*. Compared to the previously considered *Medium-size established model C*, which comes with a more comparable range of hub heights, the *Large-size recent models A and B* seem to entail fewer hours with a low capacity factor in the summer months (Figure 7c), thereby offering a slightly more consistent performance.

We unravel the identified trade-offs among turbine models by examining how their geographic location affects the capacity factor distributions. We select particular points along each turbine's hourly distribution curve in each grid cell and show which turbine performs best at this point (Figure 8). The newly introduced *Large-size recent model A @160m* performs well across various conditions. It is the best turbine overall at the 25th percentile, but it also performs well on Alpine mountain crests at the higher end of the distribution. Another newly introduced model, the *Large-size recent model B @160m*, outperforms all the others at the mean and 75th percentile of its distribution while remaining the best-performing turbine in the summer for the 90th percentile of its distribution. Finally, albeit never being the best-performing turbine in any of the considered points of the distribution, the *Medium-size recent model @120m* frequently outperforms the others in the valleys at the low end of the distribution (10th and 25th percentiles).

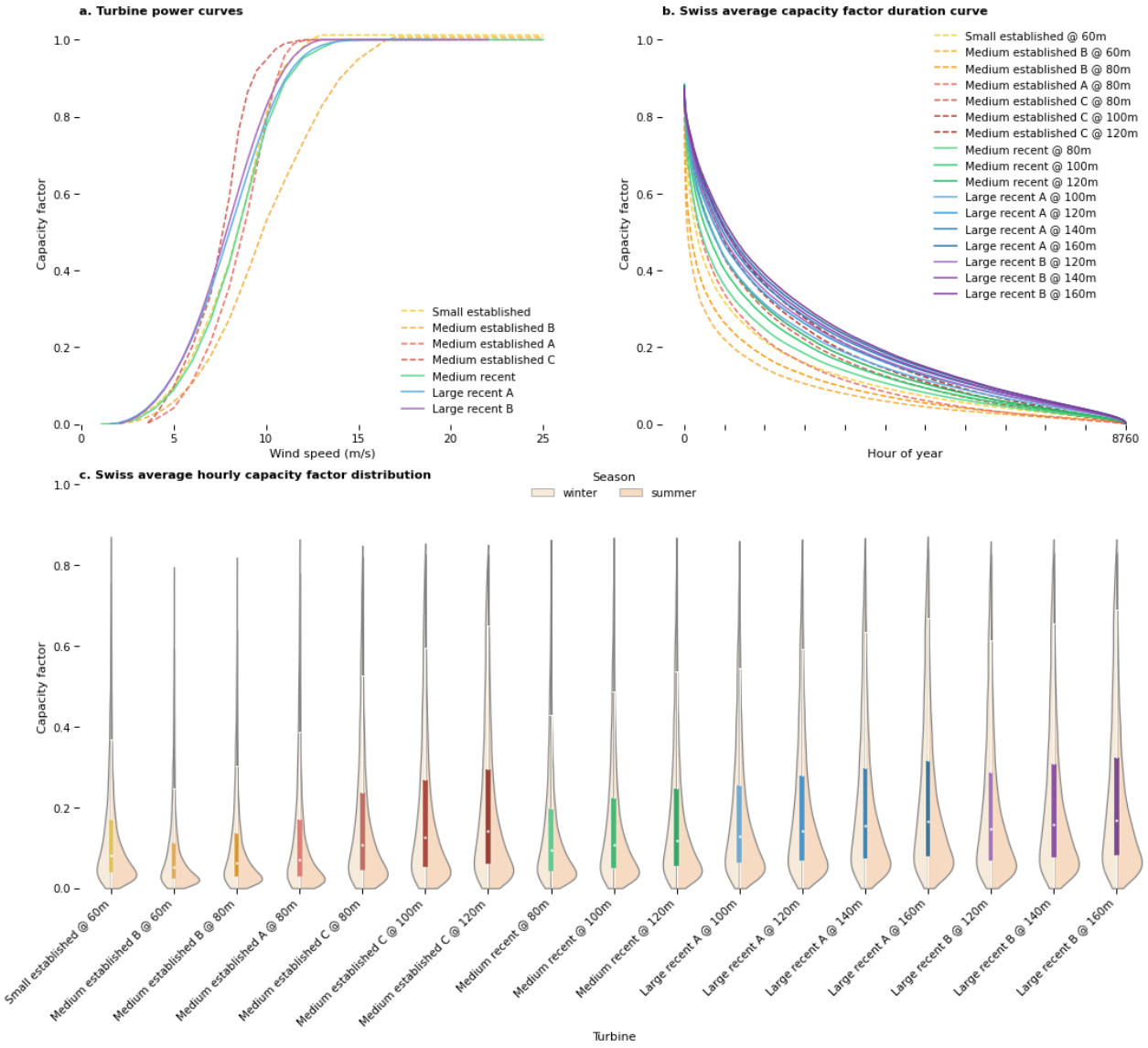

Figure 7: Turbine performance metrics of all the turbine archetypes described in Table 2 at hub heights of 60, 80, 100, 120, 140 and 160m (key: [turbine archetype] [turbine power in kW] @ [hub height]). Only turbine-hub height combinations that are relevant to the wind turbine hub height ranges have been simulated. **a.** The input turbine power curves, showing the change in turbine performance (capacity factor) with wind speed. Power curves are independent of hub height. **b.** Swiss average capacity factor duration curve for each turbine at relevant hub heights. The x-axis has been scaled from 61,320 hours (seven years) to 8,760 hours (one year). **c.** Swiss average capacity factor hourly distribution. The central box plot depicts the distribution in all 61,320 hours of data. The two violin plots depict the distribution in winter hours (Dec-Feb, left) and summer hours (Jun-Aug, right). Swiss average capacity factors are based on an area-weighted average of capacity factors in all COSMO-REA2 gridcells, where available areas per gridcell are calculated according to the method described in sub-section 2.

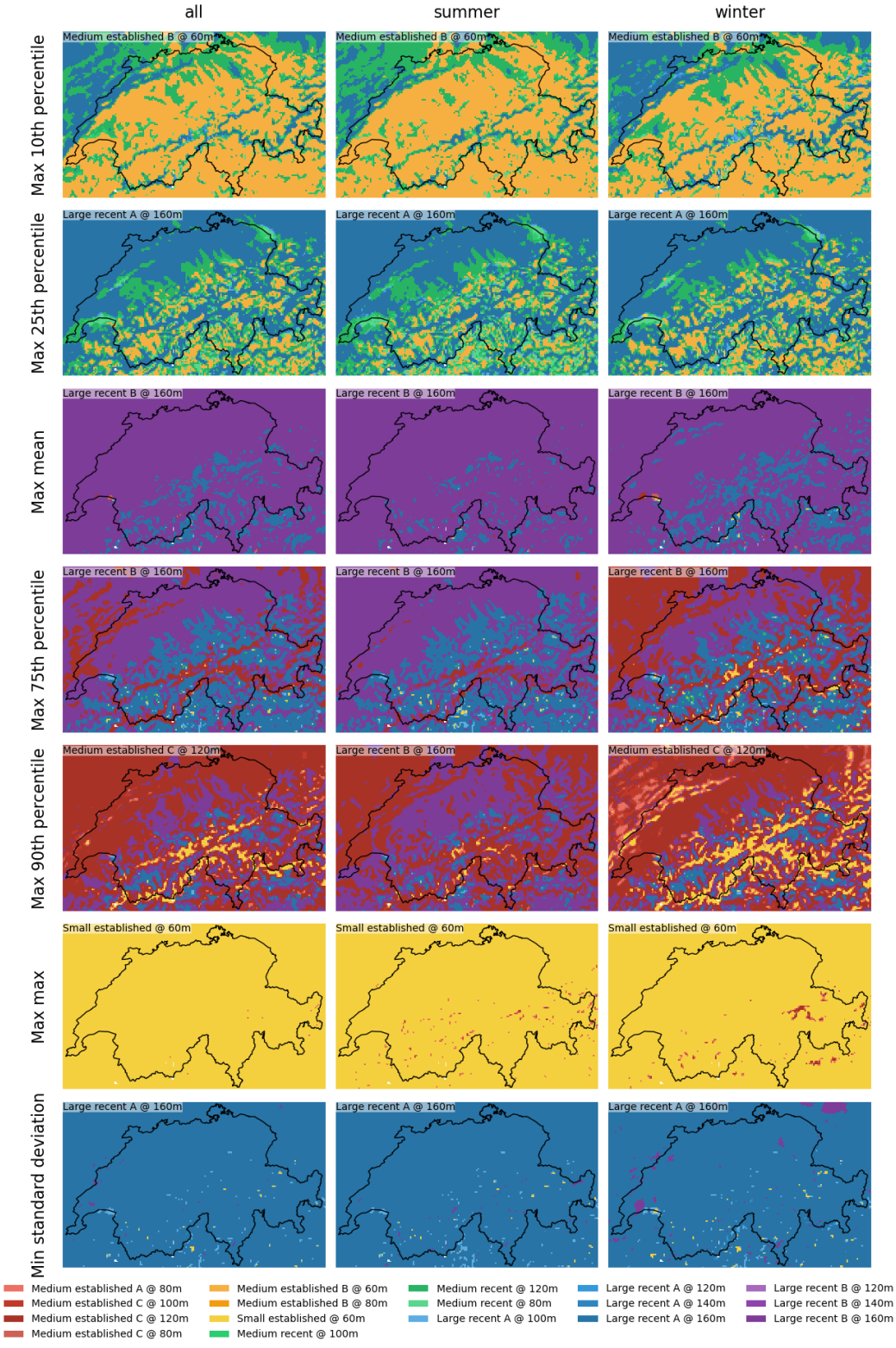

Figure 8: Best performing wind turbine in each COSMO-REA2 gridcell. Each panel shows gridcells in an oblong surrounding Switzerland, with the Swiss geographic boundary overlaid in black. Each row shows a different metric, which is taken from the hourly turbine capacity factor distribution per gridcell. We consider performance in most metrics to be 'best' when the maximum value is attained at that point in the distribution. The only exception is the scaled standard deviation ('min standard deviation'; standard deviation/mean) of the distribution, in which we consider the minimum value to be the most performant. Each column shows different temporal scopes: 'all' refers to all 61,320 hours of data, winter to hours in the months Dec-Feb, and summer to hours in the months Jun-Aug. Gridcells are coloured according to the turbine-hub height combination that performs best. In addition, the turbine-hub height combination that performs best in most Swiss gridcells is given in the top left corner of each panel.

Based on this spatio-temporal analysis of the different turbine options, we select the following turbine archetypes for further study: *Medium-size recent model @120m*, *Large-size recent model A @160m*, and *Large-size recent model B @160m*.

Having made our selection of dataset (COSMO-REA2) and wind turbine archetypes, we now must aggregate the capacity factor profiles described across Switzerland's 10,528 COSMO-REA2 gridcells into a tractable number of regions, as laid out in Appendix 8. In Figure 9a, we show the effect of clustering with k-means to produce these 65 wind turbine generation profiles for each of the four wind turbines selected in Appendix 8. For each turbine, the resulting clusters are very similar, but the resulting capacity factor profiles are quite diverse, as depicted in Figure 9b.

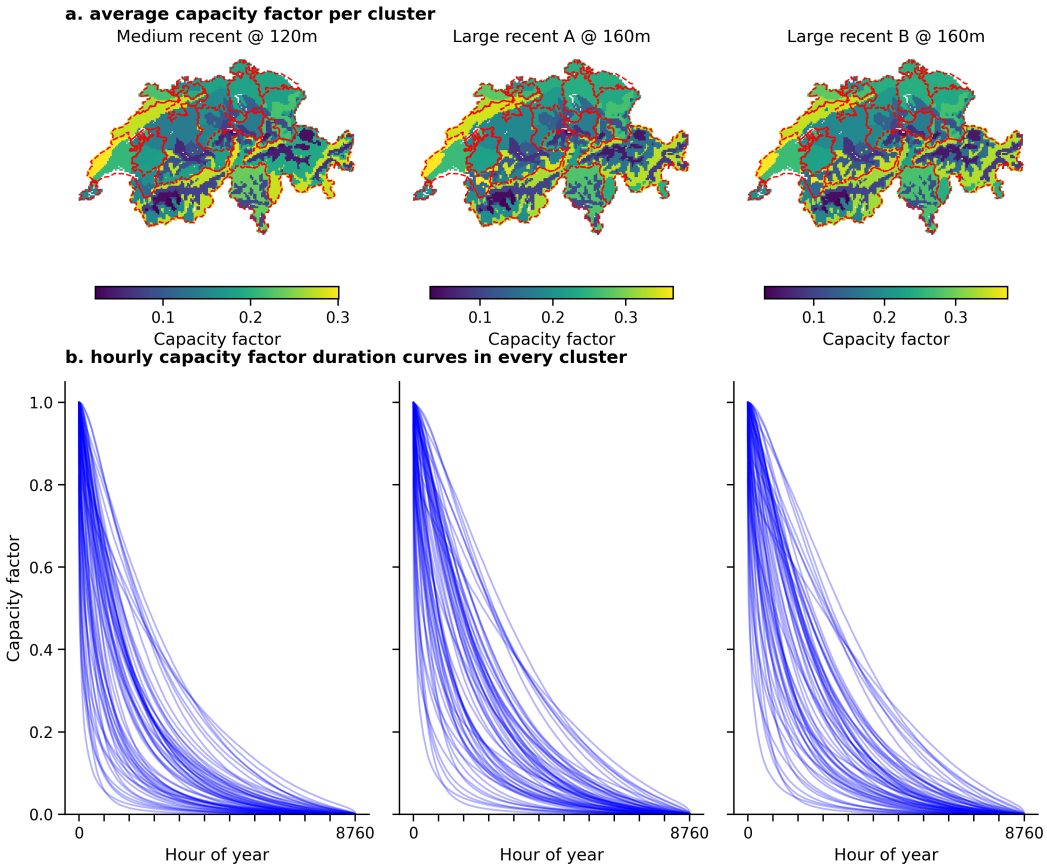

Figure 9: Result of clustering Swiss model regions into a total of 65 unique clusters based on hourly wind turbine capacity factor data derived from the COSMO-REA2 reanalysis dataset. **a.** average capacity factor per clustered region across all hours in the seven years spanned by the dataset for three turbine model archetypes. The 20 model regions are highlighted in red, but clustered regions have no borders defined since they are not strictly contiguous. **b.** Hourly capacity factor duration curve for all 65 clusters. The x-axis has been scaled from 61,320 hours (seven years) to 8,760 hours (one year). Capacity factors for each cluster are based on an area-weighted average of each underlying COSMO-REA2 gridcell.

3.2 Deployment options and contribution of wind power to a carbon-neutral Switzerland

3.2.1 Some areas are most promising for wind power, with differences across turbines

First, we look at how frequently and where each type of wind turbine is deployed as part of a carbon-neutral Swiss energy system design (Figure 10). We do so by considering all 484 design options resulting from the four 'Scenarios for generating alternatives', with varying willingness to pay and weather assumptions listed

in Table 4.

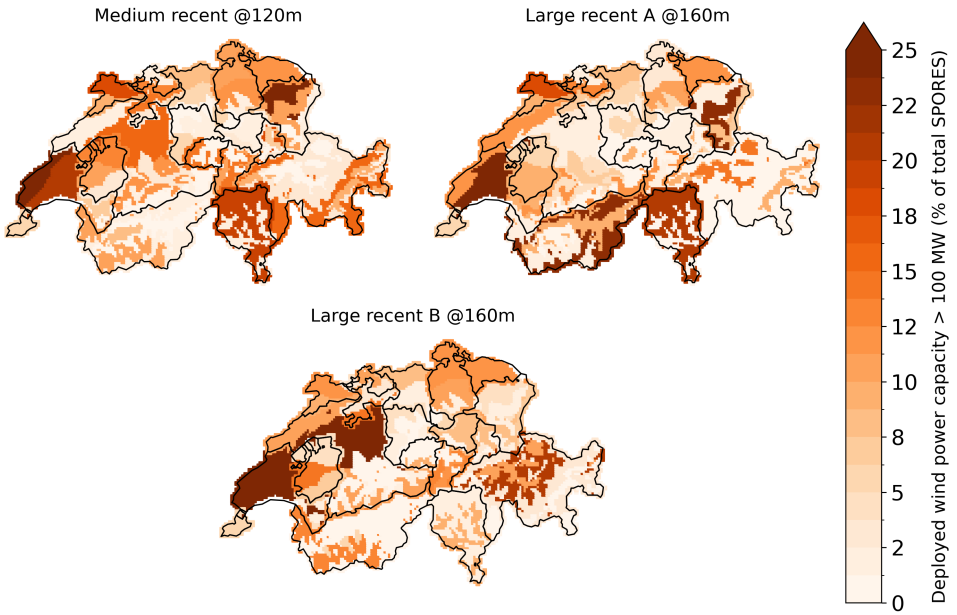

Figure 10: Frequency of wind generation capacity deployment for each considered wind turbine archetype in each of the associated 65 sub-cantonal clusters. The frequency is considered only for a deployment higher than 100 MW in any given cluster, so as to filter out the 'noise' represented by very small amounts of capacity deployment, and is provided as a percentage of occurrence across all 484 generated alternative energy system designs.

The results show that, as expected, the frequency and geographical distribution of wind power deployment across our vast option space mirrors, to a certain extent, the geographical distribution of the highest average capacity factors for each turbine, which we identified in Figure 9a. However, there are also exceptions and notable differences across turbines. For instance, the *Medium-size recent model @120m* is characterised by high capacity factors along the Jura crests belonging to the Bern and Neuchâtel cantons (Figure 9a), but is not frequently deployed there. Similarly, the two archetypes with a hub height of 160m, are not frequently deployed in the parts of Graubünden bordering Italy where capacity factors are high (Figure 9a); at the same time, they are deployed (particularly the *Large-size recent model B*) with some frequency in the innermost part of Graubünden, where capacity factors for these turbine models are in their medium-to-low range.

The occasional mismatch occurring between regions with the highest average capacity factors and regions of most frequent deployment is likely due to three factors. First, the medium-to-low range of capacity factors for the *Large-size recent model A* and *B* archetypes is between 0.1 and 0.2 (Figure 9a), which is still comparable to the highest overall capacity factors achieved by less performing

models discarded in sub-section 3.1.2. Since our SPORES algorithm tries to diversify the spatial configuration of wind deployment while remaining in the neighbourhood of the minimum feasible total system cost, it shows us that it is possible to capitalise on less windy regions (such as the innermost parts of Graubünden) by deploying these higher-performing, larger turbines. Second, our alternatives are generated across two weather years (typical and critical, as shown in Table 4), whilst capacity factors in Figure 9 are averaged across seven weather years. Discrete weather years might lead to occasional divergences in capacity factors in some regions compared to the expectations based on Figure 9. Third, we analyse wind power deployment from the perspective of a whole-energy system optimisation model. The value-added of such a model is precisely the capacity to evaluate the attractiveness of wind power generation patterns in light of their (anti)correlation with demand and other system needs in any cantonal region at high temporal resolution. From this perspective, the more frequent deployment of large turbines in apparently less-than-ideal locations could be due to a better correlation with regional or overall Swiss demand, particularly in critical moments of peak demand.

Overall, some areas stand out as particularly attractive for wind power deployment, based on the results in Figure 10. In the Jura mountains, particularly the parts in the Vaud canton, all archetypes are frequently deployed. The plateaus on both sides of the Jura mountains themselves also show promise, namely: the area around lake Geneva (Vaud canton), where all turbine models are often deployed; the part of the Swiss plateau belonging to the Bern canton, particularly attractive for the *Medium-size recent model @120m* and the *Large-size recent model B @160m*; and the small plateau in the Jura canton, favoured by the *Large-size recent model A @160m*. Some promise is also shown by clusters within the cantons Valais, Graubünden, St.Gallen-Appenzell and Ticino, with differences across turbine models as highlighted in Figure 10. Interestingly, the identified promising areas largely match those that emerged from the recent study by Spielhofer *et al.* [18], with a few exceptions. For instance, Ticino shows moderate promise in our study but less so in theirs. Differences are likely due to differences in the considered turbine archetypes, as well as to Spielhofer *et al.* [18] considering wind only as an isolated asset, without interactions with the rest of the system. In fact, Ticino had already emerged as a moderately promising area in our earlier WindVar project [8], which did consider system interactions.

3.2.2 North-South synergies exist in wind power deployment

Having identified some promising areas for wind power capacity deployment, we move on to analysing their spatial correlations across designs. We want to understand if and how cross-cantonal synergies may further inform decisions on the siting of wind turbines across the country.

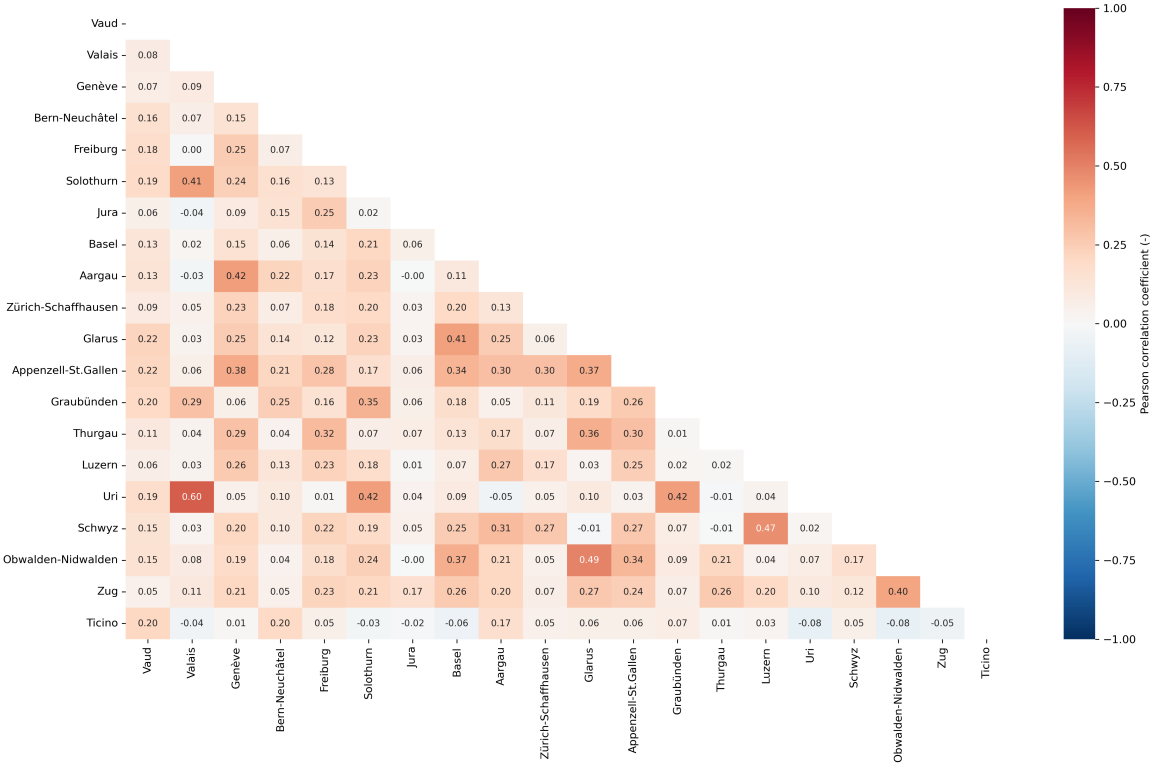

Figure 11: Spatial correlation of wind power capacity deployment across all the 484 discovered alternative energy system designs. As in Figure 10, we look only at deployments higher than 100 MW in any given region, so as to filter out the 'noise' represented by very small amounts of capacity deployment. Correlation is computed via the Pearson correlation coefficient, which assumes a linear correlation. A correlation can be either positive or negative (anti-correlation). An absolute value of the correlation coefficient higher than 0.5 indicates a strong correlation. A value between 0.3 and 0.5 indicates a moderate correlation, and one between 0 and 0.3 indicates a weak correlation.

Figure 11 shows that a few moderate and one strong correlations in wind power capacity deployment across regions do exist within our broad system design option space. Wind turbine deployment between Valais and Uri is strongly correlated and, in turn, moderately correlated with deployment in Solothurn; of these cantons, only Valais showed particular promise based on the frequency of deployment in sub-section 3.2.1. This may indicate particularly synergistic *anti-correlations* in the wind patterns between such regions that benefit system balancing. In other words, deploying turbines simultaneously in regions with particularly anti-correlated wind patterns might lead to complementary generation patterns and to an overall more stable system-wide generation profile. A few additional moderate positive correlations in wind turbine deployment emerge from Figure 11; however, we deem them less interesting as they occur between regions that appear to be characterised by substantially less frequent wind deployment in our option space, such as between Schwyz and Luzern or between

Glarus and Obwalden-Nidwalden. The identified synergies corroborate and expand the insights from our prior WindVar project [8]. In WindVar, we looked at the correlations of wind patterns across regions under the assumption that exploiting anti-correlated wind patterns could benefit system balancing. We found the most performing wind patterns to be different between the North and the South of the country, but also often across neighbouring gridcells, due to the complex terrain of the country. The synergy between Valais and Uri detected in Figure 11 matches indeed the different wind patterns identified in WindVar for gridcells within these two cantons. Similarly, it makes intuitive sense and aligns with the WindVar findings that both these southern regions have synergies with Solothurn in the North, dominated by different weather patterns. This suggests that deploying wind power simultaneously in the North and the South of the country, in particular, could lead to synergistic generation patterns and benefits for system balancing.

3.2.3 Wind power reduces reliance on solar, storage and electrolysis

As well as between regions, wind power deployment has the potential to correlate with other technologies and features in a carbon-neutral Swiss energy system. In Figure 12, we look for these possible correlations across the most relevant system design features. We ascertain that wind power experiences a strong anti-correlation with electrolyser deployment and a moderate anti-correlation with solar power, battery storage and synfuel imports. At the same time, solar power has a positive moderate correlation with electrolyser deployment and battery storage. In other words, there is a substitution effect between wind power deployment and solar power deployed alongside battery storage and electrolysers. This is in line with our expectations: a system that relies more on solar power is subject to both strong daily fluctuations (handled via battery storage) and marked seasonal variations due to the different solar irradiance between summer and winter (handled via green hydrogen from electrolysers). Investing more in wind power in place of solar power capacity, instead, returns a system which is less subject to these variations and that, in turn, also requires less storage, green hydrogen production capacities and synfuel imports.

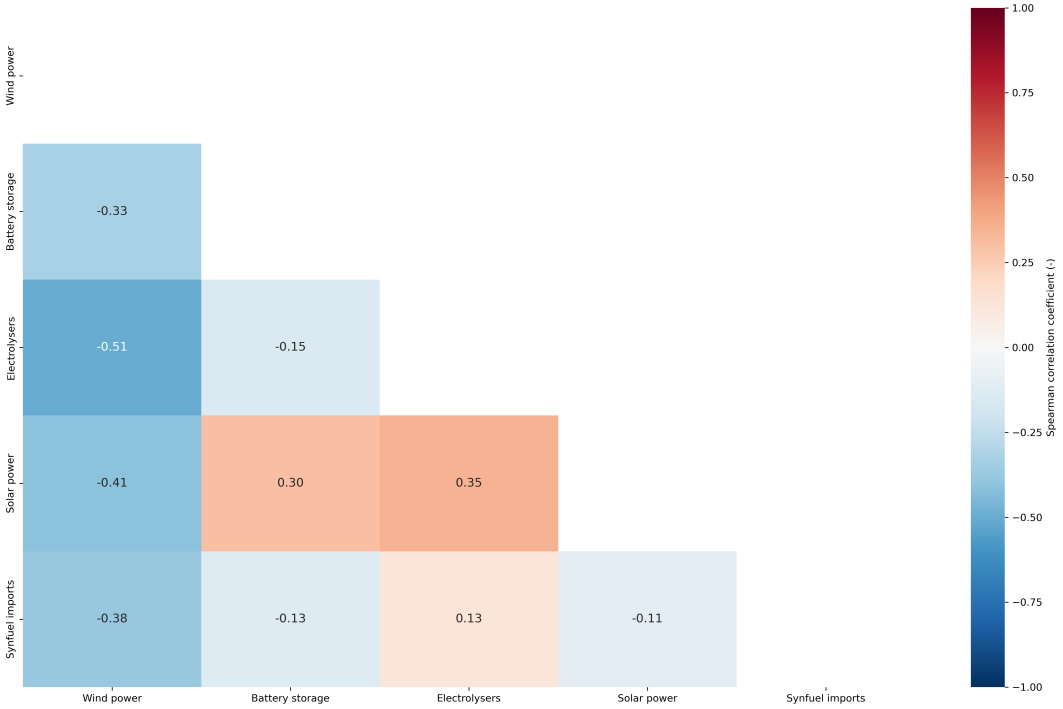

Figure 12: Correlation among key system design features: renewable generation capacity (solar and wind), battery storage, electrolysers (which can be interpreted as a proxy for a system relying more on e-fuels and long-term storage), electricity grid expansion, and reliance on imported synfuels. Correlations are across all the 484 discovered alternative energy system designs and, unlike in Figure 11, are here computed by means of the Spearman correlation coefficient. In fact, the Spearman correlation coefficient is more suited when the correlation is not expected to be linear, which applies to most of the system features considered here. For instance, an increase in renewable power capacity is likely to lead to an increased need for storage, but not linearly. A correlation can be either positive or negative (anti-correlation). An absolute value of the correlation coefficient higher than 0.5 indicates a strong correlation. A value between 0.3 and 0.5 indicates a moderate correlation, and one between 0 and 0.3 indicates a weak correlation.

3.3 Representative wind-based system designs and uncertainty-aware performance comparison

The findings so far provide us with a good picture of which locations might be most interesting for wind power deployment in Switzerland, which synergies across locations might be worth pursuing, and how a push for strategic wind power deployment could impact the carbon-neutral Swiss energy system overall. Based on these findings, we aim to select a few representative options for wind power deployment that may capture the most interesting solutions that have emerged so far, so that we may further analyse those in light of uncertainty.

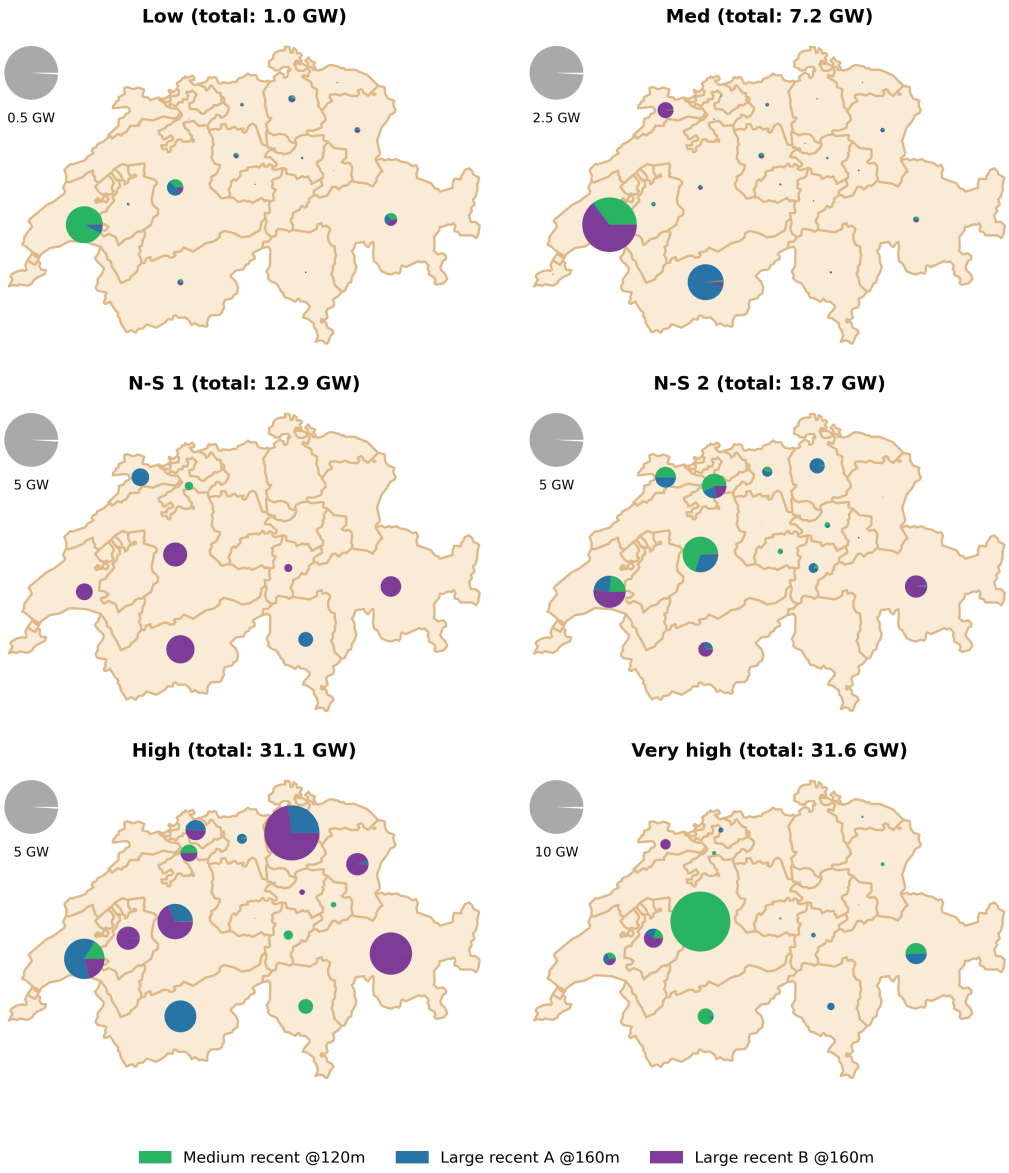

Figure 13: Selected representative wind power deployment options for further uncertainty testing. Here, wind power capacity is spatially aggregated at the level of near-cantonal model regions for better readability. The total Swiss wind capacity increases progressively from options 'Low' to 'Very high'. The 'N-S 1' and 'N-S 2' labels emphasise the reliance on different possible North-South synergies in wind deployment, as identified in sub-section 3.2. In the top-left corner of each sub-figure, a legend clarifies what wind power capacity is represented by a pie-chart of maximum size within each map.

To this end, we select six representative system design options from our option space by looking at different percentiles of total wind power capacity deployment in the system, namely: 0^{th}, 25^{th}, 50^{th}, 75^{th}, 90^{th} and 95^{th}. This way, we make sure to represent progressively higher amounts of wind power in the system, from the minimum to the near-highest amount in our option space. Hence, we assess whether such percentiles cover the aspects of interest identified in the previous sections in terms of promising regions and synergistic deployment. If not, we make corrections by looking for an alternative system design option with wind capacity closest to a given percentile that may provide the features of interest. As a result, we identify the six configurations in Figure 13 as the most useful for further analysis.

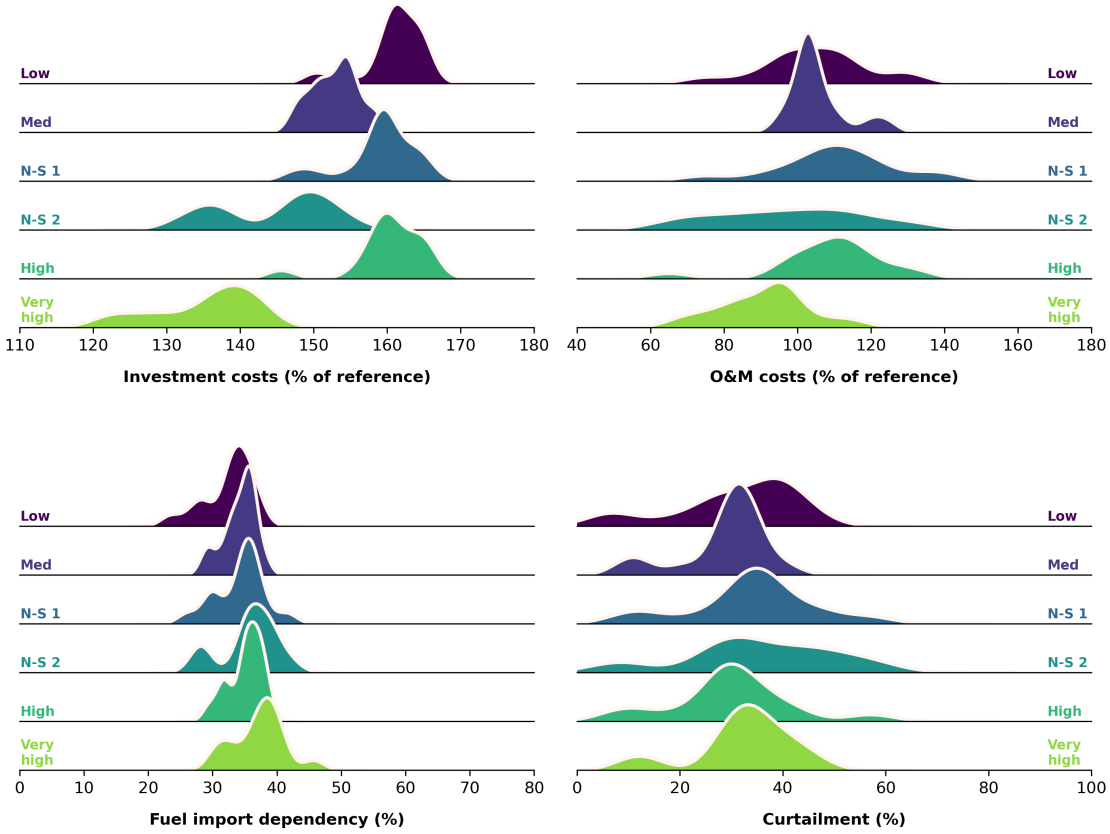

Figure 14: Performance comparison for the six selected representative wind and energy system designs based on probability density functions. The probabilistic performance is based on out-of-sample testing across sixteen varying weather and neighbouring-country conditions, as outlined in Table 4. Investment-cost and O&M-cost performances are quantified with respect to the lowest-cost performance observed within the whole first-stage option space for any given fixed boundary conditions. Fuel import dependency is calculated as synthetic-fuel imports percentage in the total primary energy supply. Curtailment is calculated for the whole system, including solar and wind capacity. All metrics are specific to the Swiss system, even though other neighbouring countries are modelled.

The ‘Low’ wind power design is characterised by a low and homogeneously spread out wind power capacity, with larger hubs in the cantons Vaud, the combined region Bern-Neuchâtel, and Graubünden, a mix of turbine archetypes slightly dominated by the *Medium-size recent model @120m*. The ‘Med’ option deploys a diverse mix of turbines, with two key hubs in Vaud and Valais, and a smaller one in Jura. Option ‘N-S 1’ concentrates a mix of turbines dominated by the *Large-size recent model B @160m* across Ticino and Valais in the South, Vaud, Uri, Bern-Neuchâtel and Graubünden in the Centre, and Solothurn and Jura in the North. This comprises the cantons we identified in sub-section 3.2 as particularly interesting due to their seemingly strong synergy in wind power deployment across our option space, and complements those with other neighbouring cantons also building on North-South synergies. Similarly, option ‘N-S 2’ captures the North-South deployment synergy we discovered between Uri, Valais and Solothurn, while also supporting it with substantial capacity in the Bern-Neuchâtel, Vaud and Jura regions; this second N-S configuration is, however, particularly dominated by the *Medium-size recent model @120m* archetype. Option ‘High’ represents a high wind power deployment scenario, including a high capacity share in previously underexplored locations, such as the Zürich, Fribourg and St.Gallen-Appenzell regions. Finally, option ‘Very high’ provides the highest deployment of the smallest considered turbine archetype, the *Medium-size recent model @120m*, as well as the highest deployment overall. It capitalises heavily on the large land availability in the Bern-Neuchâtel region (see Figure 2), but also on some of the other areas identified as promising in sub-section 3.2, such as Valais and Graubünden.

Figure 14 shows the outcomes of the out-of-sample testing of the selected configurations across the sixteen uncertain conditions identified in Table 4. The resulting probability density functions should be interpreted as follows: narrower distributions with pronounced peaks mean less variation (i.e., higher robustness) in the performance of a given metric across the set of tested conditions. In addition, the position of the peak provides an idea of the most frequent score for a given metric. We see that all configurations take advantage of the marginal relaxation allowed for (dis)investments in capacity to deal with out-of-sample conditions, as we expected. Interestingly, configurations with a medium-high (‘N-S 2’) to high (‘Very high’) wind power capacity dominated by the *Medium-size recent model @120m*, with large hubs in Bern-Neuchâtel, often require a smaller total extent of capacity adjustments than the others; at the same time, they have overall lower peaks in investment cost in their distribution, which means they are less consistent in how they adjust to boundary condition changes. The ‘N-S 2’ and ‘Very High’ configurations confirm their limited consistency also for operation costs, but this time, they are closely followed by all the other configurations except for the ‘Medium’ one, which emerges as substantially more consistent. The exceptionally consistent results of the ‘Medium’ configuration, further corroborated by the good performance in terms of curtailment, may result from the well-balanced mix of turbines deployed across the North-South axis. The ‘High’ wind configuration is the second-most stable across all indicators. This configuration is mostly dominated by the two *Large-size recent* turbine archetypes and capitalises on the North-South synergy while also having hotspots in a diverse set of regions. Still,

complementing the deployment of turbines along the North-South axis with other hotspots, albeit necessary, does not seem to be a sufficient condition to ensure robust performances. In fact, the 'N-S 2', which has a similar spatial configuration of wind turbine deployment but relies mainly on the *Medium-size recent model @120m* archetype, performs less robustly than the 'High' configuration across all indicators, albeit requiring lower investment costs. This suggests that, while capitalising on the North-South correlation is a robust design choice for an energy system based on the two *Large-size recent @160m* turbine archetypes, the same might not apply for a system dominated by a *Medium-size recent @120m* archetype. This aligns with the finding from section 3.1.2, where the *Medium-size recent model @120m* emerged as promising in peculiar conditions and areas but not overall; this might explain the greater sensitivity to varying boundary conditions in configurations dominated by this turbine archetype. We also see that performance differences in terms of fuel import dependency are marginal, with the 'Medium' and 'High' system configurations being only slightly more robust for varying boundary conditions. This mitigates the importance of the correlation between higher wind deployment and reduced synfuel imports found in Figure 12; arguably, changes in external boundary conditions, such as wind patterns and different planning choices in neighbouring countries, have a greater role in determining the extent of the required fuel imports in Switzerland, which remain in a relatively narrow range regardless of the chosen internal wind power configuration. Nonetheless, such imports never exceed 45% of the primary energy supply, with tails as low as 23% in favourable conditions.

4 Conclusion

With this project, we set out to discover possible configurations of wind power within a future carbon-neutral Swiss energy system and analyse their trade-offs. On the way to this goal, we first identified the most promising turbine models for Swiss wind patterns. Second, we integrated those and the associated capacity factor profiles in a high-resolution energy system model that generates near-optimal Swiss system design alternatives, to discover and analyse the design space for wind power deployment in the framework of the Swiss energy transition. Third and final, we identified some representative solutions within this broad option space and further analysed their respective merits against the uncertainty of weather and design conditions in neighbouring European countries. In light of this analysis, we synthesise several findings and insights that are relevant to both research and policy.

Our study showed that the COSMO-REA2 and NEWA datasets have relative strengths and weaknesses. However, COSMO-REA2 better represents measured data and observed peaks in Swiss winds during summer afternoons, which are interesting as they tend to anti-correlate with wind patterns in neighbouring countries. Therefore, we selected COSMO-REA2 data for our analysis, as we did in our previous WindVar project [8], and recommend this dataset for studies that look at Swiss wind also in the context of possible synergistic wind deployment choices in neighbouring countries.

Using COSMO-REA2, we then quantified the trade-offs among many turbine archetypes based on commercially available turbine models that either have been previously tested in Switzerland or have particularly promising features for Swiss wind patterns. We found the most interesting performances in the archetypes we named *Medium-size recent model @120m*, *Large-size recent model A @160m* and *Large-size recent model B @160m*, which showed better or more versatile capacity factors across Swiss orography compared to other archetypes. We advise future studies or pilot wind deployment projects to concentrate on these types of turbines and hub heights.

Having integrated these turbine archetypes within our Swiss energy system model, we discovered that some differences exist across turbines in terms of where their deployment can be most beneficial for the system. To a large extent, we see that each turbine model is most frequently deployed within our option space in areas where its respective capacity factor is highest. Nonetheless, we also see that it is possible to capitalise on less windy regions (such as the innermost parts of Graubünden) by deploying higher-performing, larger turbines, such as the two archetypes with a hub height of 160m.

Overall, some areas appear as most promising for wind power deployment. First, the Jura crests, particularly across the Vaud and Solothurn cantons. Second, the plateaus on both sides of the Jura crests: around Lake Geneva; within the canton of Bern; and the small plateau in the Jura canton. Third and final, areas within the cantons Valais, Graubünden St.Gallen-Appenzell and Ticino, with differences across turbine models. These most-promising areas include but also expand those identified in a recent study [18] and in our previous WindVar project [8]. This is a direct benefit of the broader range of technically-feasible and economically-comparable wind deployment options we generated via SPORES, which highlights how deployment could be attractive in previously unexplored regions with near-optimal economic value. In addition, our results largely match and corroborate those that emerged from the recent study by Spielhofer *et al.*, which used substantially different methods.

We also show that deployment in some areas positively correlates, revealing synergistic patterns that may be leveraged for system balancing. In particular, deployment in the Southern Alpine cantons of Valais and Uri correlates with deployment in the Northern canton of Solothurn, revealing the benefits of integrating different wind regimes in the system at once. In general, a higher deployment of wind, which capitalises on synergies across the diverse territory of Switzerland, leads to a reduced need for solar power. We find many feasible and cost-comparable system designs with relative contributions from wind and solar varying from negligible to dominant, which means there is a large flexibility of choice in deciding how much to rely on the two technologies. In addition to this expected technological trade-off, we find that strategic wind power deployment can also reduce the need for additional pieces of infrastructure for system balancing, such as storage and electrolysis capacity. It is the task of decision-makers to evaluate the extent to which these system-balancing benefits may compensate for the likely lower social acceptability of wind turbines compared to solar panels.

Our testing of representative wind deployment options across many uncertain

future operating conditions sheds further light on the above findings. Capitalising on turbine deployment along the North-South axis and complementing it with a diverse set of wind power hotspots across other cantons appears as a robust design choice, but only when based primarily on the large turbine archetypes with a hub height of 160m. When a similar configuration is dominated by the *Medium-size recent model @120m*, the system performs well, and for some indicators even better, on average, but its performance is substantially more sensitive to changes of (uncontrollable) boundary conditions, such as weather patterns and planning decisions in neighbouring countries. This confirms, on the one hand, the better performance of the *Large-size recent models A and B* while, on the other hand, corroborating the importance of a diverse siting and mixed portfolio of wind farms. The most robust system designs are those where wind power is deployed in large enough amounts to cover the key synergistic areas North-South together with hotspots in other individually promising regions, with each region capitalising on the turbine type most suitable for their local weather regimes.

Overall, our findings show that there is a large techno-economic potential for wind power to be part of a future Swiss energy system. Compared to solar, system designs relying more on wind power show additional technical benefits, such as a reduced need for storage and electrolysis capacity and higher robustness against the uncertainty of boundary conditions. As solar is typically met with higher social acceptability, policymakers should decide on these trade-offs.

5 Outlook and next steps

Our work highlights some concrete, promising options in terms of turbine models and deployment areas for wind power to contribute to the Swiss energy transition. What is more, we generated hundreds of alternative deployment options that deviate either marginally or substantially from the most promising ones and may allow for accommodating further stakeholder preferences. Future work should look at stakeholder preferences more in-depth, letting stakeholders engage interactively with the space of design options we generated with the aim of identifying a consensus solution. Should the existing space of design option not suffice to meet conflicting stakeholder preferences, one could use the elicited preferences to further perfect the search for practically viable wind deployment options. In fact, the SPORES algorithm used in this work to generate the design options lends itself to a human-in-the-loop (HIL) approach, in which stakeholder preferences collected in a first round of engagement are used to refine and expand the space of feasible design options. We hypothesise that this would ensure a high degree of success in a second stakeholder engagement round in identifying a consensus solution for practical implementation.

In parallel, future work should focus on devising incentive schemes to favour capacity deployment in the locations identified, together with stakeholders, as the most desirable for wind power.

It would also be useful to expand the analysis to more weather years, making our testing of system operation against uncertain weather conditions even more

solid. For this, we advocate further development of the COSMO-REA2 dataset. Moreover, it is important to study the future possible evolution of weather due to climate change, which may substantially deviate from historical patterns, especially regarding hydroelectric production and the role that wind power may have in counterbalancing the latter.

6 National and international cooperation

The characterisation of the Swiss energy system within our Calliope modelling framework was informed by the concluded CH2040 and the ongoing SWEET PATHFNDR projects, and by the collaboration with the Nexus-e team at ETH Zürich in both these projects.

7 Acknowledgements

The calculations were run on the Euler cluster of ETH Zürich for the first part of the analysis concerning wind power potential and turbine performance, and on the DelftBlue supercomputer of TU Delft for the second part concerning deployment options and contribution of wind power to a carbon-neutral Switzerland.

References

[1] B. Pickering, C. M. Grams and S. Pfenninger, "Sub-national variability of wind power generation in complex terrain and its correlation with large-scale meteorology," en, *Environmental Research Letters*, vol. 15, no. 4, p. 044 025, 2020, Publisher: IOP Publishing, ISSN: 1748-9326. DOI: 10.1088/1748-9326/ab70bd. [Online]. Available: https://dx.doi.org/10.1088/1748-9326/ab70bd (visited on 26/06/2023).

[2] C. M. Grams, R. Beerli, S. Pfenninger, I. Staffell and H. Wernli, "Balancing Europe's wind-power output through spatial deployment informed by weather regimes," en, *Nature Climate Change*, vol. 7, no. 8, pp. 557–562, 2017, Number: 8 Publisher: Nature Publishing Group, ISSN: 1758-6798. DOI: 10.1038/nclimate3338. [Online]. Available: https://www.nature.com/articles/nclimate3338 (visited on 26/06/2023).

[3] F. Lombardi, B. Pickering, E. Colombo and S. Pfenninger, "Policy Decision Support for Renewables Deployment through Spatially Explicit Practically Optimal Alternatives," English, *Joule*, vol. 4, no. 10, pp. 2185–2207, 2020, Publisher: Elsevier, ISSN: 2542-4785, 2542-4351. DOI: 10.1016/j.joule.2020.08.002. [Online]. Available: https://www.cell.com/joule/abstract/S2542-4351(20)30348-2 (visited on 26/06/2023).

[4] S. Pfenninger, "Dealing with multiple decades of hourly wind and PV time series in energy models: A comparison of methods to reduce time resolution and the planning implications of inter-annual variability," en, *Applied Energy*, vol. 197, pp. 1–13, 2017, ISSN: 0306-2619. DOI: 10.1016/j.apenergy.2017.03.051. [Online]. Available: https://www.sciencedirect.com/science/article/pii/S0306261917302775 (visited on 26/06/2023).

[5] B. Pickering and R. Choudhary, "Quantifying resilience in energy systems with out-of-sample testing," en, *Applied Energy*, vol. 285, p. 116 465, 2021, ISSN: 0306-2619. DOI: 10.1016/j.apenergy.2021.116465. [Online]. Available: https://www.sciencedirect.com/science/article/pii/S0306261921000313 (visited on 26/06/2023).

[6] I. Staffell and S. Pfenninger, "Using bias-corrected reanalysis to simulate current and future wind power output," en, *Energy*, vol. 114, pp. 1224–1239, 2016, ISSN: 0360-5442. DOI: 10.1016/j.energy.2016.08.068. [Online]. Available: https://www.sciencedirect.com/science/article/pii/S0360544216311811 (visited on 26/06/2023).

[7] S. Jafari, T. Sommer, N. Chokani and R. S. Abhari, "Wind Resource Assessment Using a Mesoscale Model: The Effect of Horizontal Resolution," en, American Society of Mechanical Engineers Digital Collection, 2013, pp. 987–995. DOI: 10.1115/GT2012-69712. [Online]. Available: https://dx.doi.org/10.1115/GT2012-69712 (visited on 26/06/2023).

[8] B. Pickering and S. Pfenninger, *WindVar. Spatial-temporal variability of wind energy potential in Switzerland and neighbouring countries (Project report No. SI/501768)*, 2020. [Online]. Available: https://www.aramis.admin.ch/Default?DocumentID=66408&Load=true.

[9] M. Dörenkämper *et al.*, "The Making of the New European Wind Atlas – Part 2: Production and evaluation," English, *Geoscientific Model Development*, vol. 13, no. 10, pp. 5079–5102, 2020, Publisher: Copernicus GmbH, ISSN: 1991-959X. DOI: 10.5194/gmd-13-5079-2020. [Online]. Available: https://gmd.copernicus.org/articles/13/5079/2020/ (visited on 26/06/2023).

[10] A. N. Hahmann *et al.*, "The making of the New European Wind Atlas – Part 1: Model sensitivity," English, *Geoscientific Model Development*, vol. 13, no. 10, pp. 5053–5078, 2020, Publisher: Copernicus GmbH, ISSN: 1991-959X. DOI: 10.5194/gmd-13-5053-2020. [Online]. Available: https://gmd.copernicus.org/articles/13/5053/2020/ (visited on 26/06/2023).

[11] S. Wahl *et al.*, "A novel convective-scale regional reanalysis COSMO-REA2: Improving the representation of precipitation," en, *Meteorologische Zeitschrift*, pp. 345–361, 2017, Publisher: Schweizerbart'sche Verlagsbuchhandlung, ISSN: , DOI: 10.1127/metz/2017/0824. [Online]. Available: https://www.schweizerbart.de/papers/metz/detail/26/87333/A_novel_convective_scale_regional_reanalysis_COSMO?af=crossref (visited on 26/06/2023).

[12] C. Bauer *et al.*, *Electricity storage and hydrogen – technologies, costs and impacts on climate change*. 2022.

[13] B. Pickering, F. Lombardi and S. Pfenninger, "Diversity of options to eliminate fossil fuels and reach carbon neutrality across the entire European energy system," English, *Joule*, vol. 6, no. 6, pp. 1253–1276, 2022, Publisher: Elsevier, ISSN: 2542-4785, 2542-4351. DOI: 10.1016/j.joule.2022.05.009. [Online]. Available: https://www.cell.com/joule/abstract/S2542-4351(22)00236-7 (visited on 26/06/2023).

[14] T. Tröndle, S. Pfenninger and J. Lilliestam, "Home-made or imported: On the possibility for renewable electricity autarky on all scales in Europe," en, *Energy Strategy Reviews*, vol. 26, p. 100 388, 2019, ISSN: 2211-467X. DOI: 10.1016/j.esr.2019.100388. [Online]. Available: https://www.sciencedirect.com/science/article/pii/S2211467X19300811 (visited on 03/07/2023).

[15] *Europe's onshore and offshore wind energy potential — European Environment Agency*, en, Publication. [Online]. Available: https://www.eea.europa.eu/publications/europes-onshore-and-offshore-wind-energy-potential (visited on 26/06/2023).

[16] J. Dujardin, A. Kahl and M. Lehning, "Synergistic optimization of renewable energy installations through evolution strategy," en, *Environmental Research Letters*, vol. 16, no. 6, p. 064 016, 2021, Publisher: IOP Publishing, ISSN: 1748-9326. DOI: 10.1088/1748-9326/abfc75. [Online]. Available: https://dx.doi.org/10.1088/1748-9326/abfc75 (visited on 26/06/2023).

[17] F. Lombardi, B. Pickering and S. Pfenninger, "What is redundant and what is not? Computational trade-offs in modelling to generate alternatives for energy infrastructure deployment," en, *Applied Energy*, vol. 339, p. 121 002, 2023, ISSN: 0306-2619. DOI: 10.1016/j.apenergy.2023.121002. [Online]. Available: https://www.sciencedirect.com/science/article/pii/S0306261923003665 (visited on 03/07/2023).

[18] R. Spielhofer, J. Schwaab and A. Grêt-Regamey, “How spatial policies can leverage energy transitions Finding Pareto-optimal solutions for wind turbine locations with evolutionary multi-objective optimization,” en, *Environmental Science & Policy*, vol. 142, pp. 220–232, 2023, ISSN: 1462-9011. DOI: 10.1016/j.envsci.2023.02.016. [Online]. Available: https://www.sciencedirect.com/science/article/pii/S1462901123000497 (visited on 04/07/2023).

[19] T. Brown, D. Schlachtberger, A. Kies, S. Schramm and M. Greiner, “Synergies of sector coupling and transmission reinforcement in a cost-optimised, highly renewable European energy system,” en, *Energy*, vol. 160, pp. 720–739, 2018, ISSN: 0360-5442. DOI: 10.1016/j.energy.2018.06.222. [Online]. Available: https://www.sciencedirect.com/science/article/pii/S036054421831288X (visited on 26/06/2023).

[20] C. E. Fleischer, “A data processing approach with built-in spatial resolution reduction methods to construct energy system models,” en, *Open Research Europe*, vol. 1, p. 36, 2022, ISSN: 2732-5121. DOI: 10.12688/openreseurope.13420.2. [Online]. Available: https://open-research-europe.ec.europa.eu/articles/1-36/v2 (visited on 26/06/2023).

[21] T. Tröndle, J. Lilliestam, S. Marelli and S. Pfenninger, “Trade-Offs between Geographic Scale, Cost, and Infrastructure Requirements for Fully Renewable Electricity in Europe,” en, *Joule*, vol. 4, no. 9, pp. 1929–1948, 2020, ISSN: 2542-4351. DOI: 10.1016/j.joule.2020.07.018. [Online]. Available: https://www.sciencedirect.com/science/article/pii/S2542435120303366 (visited on 11/11/2021).

[22] M. Hoffmann, L. Kotzur, D. Stolten and M. Robinius, “A Review on Time Series Aggregation Methods for Energy System Models,” en, *Energies*, vol. 13, no. 3, p. 641, 2020, Number: 3 Publisher: Multidisciplinary Digital Publishing Institute, ISSN: 1996-1073. DOI: 10.3390/en13030641. [Online]. Available: https://www.mdpi.com/1996-1073/13/3/641 (visited on 26/06/2023).

[23] L. Kotzur, P. Markewitz, M. Robinius and D. Stolten, “Impact of different time series aggregation methods on optimal energy system design,” en, *Renewable Energy*, vol. 117, pp. 474–487, 2018, ISSN: 0960-1481. DOI: 10.1016/j.renene.2017.10.017. [Online]. Available: https://www.sciencedirect.com/science/article/pii/S0960148117309783 (visited on 26/06/2023).

[24] C. P. Ruiz *et al.*, *The JRC-EU-TIMES model. Bioenergy potentials for EU and neighbouring countries*, en, ISBN: 9789279538803 9789279538797 ISSN: 1018-5593, 1831-9424, 2015. DOI: 10.2790/01017. [Online]. Available: https://publications.jrc.ec.europa.eu/repository/handle/JRC98626 (visited on 26/06/2023).

8 Appendix - defining spatial clusters

Capacity factor profiles emerging from the analysis in sub-section 2.1.2 are gridcell specific, leading to tens of thousands of profiles that need to be synthesised into a tractable number of regions; no more than 200 profiles across all turbines can be realistically used as model inputs. To cluster spatial regions, we will take an area-weighted average across groups of gridcells. Usually, gridcells are grouped by administrative regions, such as countries [19, 20, 21]. In Switzerland, we could feasibly aggregate to the cantonal level, but this risks smoothing out the very spatiotemporal features we are hoping to capture. Nevertheless, a cantonal representation of our wind turbines will match the regionalisation of Switzerland we use to describe the rest of the energy system (20 regions that are mostly cantonal, with some representing merged cantons; see sub-section 2.2).

This appendix describes how we cluster gridcells in each model region. One option is to use sub-cantonal administrative regions. For instance, we could group Swiss cantonal districts, of which there are 169, based on those which are most similar in wind turbine performance. However, districts are not well placed to spatially resolve the meteorological phenomena affecting wind turbine performance. Those in the Alps tend to include valleys and surrounding peaks, leading to mountain-valley flows effectively cancelling each other out in the resulting profile. Rather than use sub-cantonal administrative regions, we instead allow the similarities in the temporal profiles of each gridcell to speak for themselves by clustering algorithmically. This mitigates possible issues with combining very dissimilar capacity factor profiles. However, different clustering algorithms will tell different stories, so it is necessary to compare their relative merits.

Therefore, as shown in Figure 15, we test the effect of clustering with two well-known unsupervised algorithms: Spectral clustering and k-means[3]. K-means is a commonly used algorithm when clustering energy systems data [22, 23, 4]. With Spectral clustering, the input data is decomposed into components that describe its key features (e.g. seasonal variations) and those components are then clustered using k-means. To asses both algorithms, we cluster using Vestas V110 @ 120m capacity factors using the full temporal (hourly) and spatial (2km) resolution of the COSMO-REA2 dataset (approximately 650 million data points within Switzerland).

At no point do we provide the algorithm with information on the geographic location of gridcells. Yet, both clustering methods expose the orography of Switzerland. With k-means clusters, Alpine crests and valleys tend to be grouped separately. With Spectral clustering, the result is more spatially contiguous. These clusters also match Swiss orography - such as a separation between the Swiss plateau, northern pre-Alps, Alps, and the southern pre-Alps. However, Spectral clustering undervalues high spatio-temporal resolution variations such as mountain-valley flows; the contiguous clusters suggest the dominance of longer time-scale features of the timeseries. Based on the ability for k-means to better identify mountains and valleys, we deem it a more useful algorithm for our case.

[3] We use the Python package scikit-learn to undertake our clustering. To find out more about each algorithm, we refer to their documentation: https://scikit-learn.org/stable/modules/clustering.html

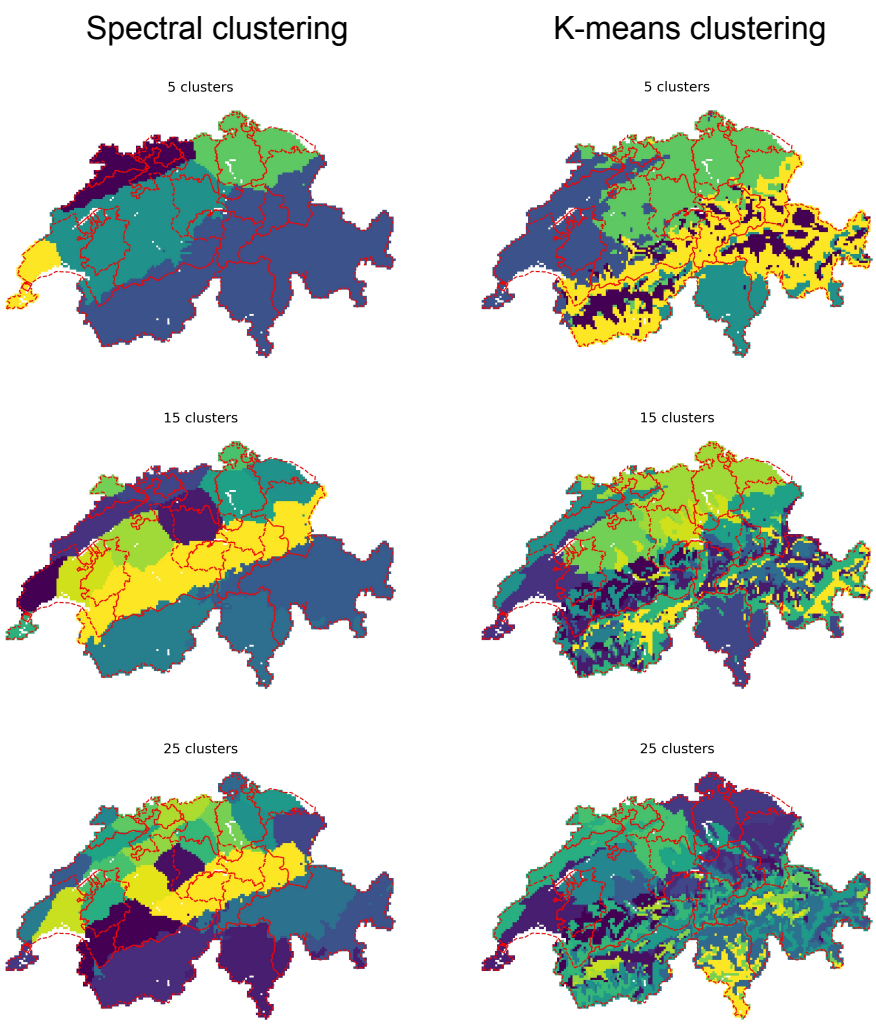

Figure 15: Swiss spatial clusters identified by applying two clustering algorithms to hourly capacity factors derived from COSMO-REA2 wind speeds. Capacity factors are simulated using the Vestas V110 turbine with a hub height of 120m. The capacity factor in each gridcell is normalised relative to its long-term average before undertaking clustering, to focus clustering on the shape of the temporal profile. Cluster colours have no significance and only differentiate different clusters. Overlaid in red on each panel are the boundaries of the 20 regions used in our model (see sub-section 2.2), which predominantly match cantonal borders.

Not all model regions are equally meteorologically diverse. Therefore, we want a different number of clusters per model region to capture the effect of different meteorological phenomena with the minimum number of total Swiss clusters. We could make this differentiation using heuristics such as the number of districts or the relative share of land area available for wind deployment. However, these have no bearing on wind turbine generation. Instead, we use the identified

clusters from our algorithmic methods. With both methods, Figure 15 shows how Swiss administrative borders[4] often do not match clusters. This is less the case with Spectral clustering, where key administrative boundaries described by mountain crests (northern Valais, Graubünden, and Ticino borders) are well-matched by clusters. However, in the Swiss Plateau, where administrative borders are less dictated by orography, there is no match with the boundaries of either clustering method.

Table 5 shows the result of this mismatch. Using k-means, there are 82 unique clusters per Swiss region when representing the entirety of Switzerland with 25 clusters. This mismatch enables us to understand how spatially differentiated each canton is. We define a number of clusters to generate algorithmically per region based on the range of unique clusters defined in Table 5. This is a trade-off between the two algorithms, the number of unique clusters at different levels of Swiss-wide clustering, and the number of wind turbine profiles we can handle in our model. The resulting selection leads to 65 clusters in total, with up to five clusters in a single model region. Although larger model regions tend to have more clusters, the resulting number of clusters per region has a Pearson correlation coefficient of only 0.2 with regional available wind generation land area.

		Number of unique clusters representing >90% gridcells per modelled region (spectral | k-means)																			
		1	2	3	4	5	6	7	8	9	10	11	12	13	14	15	16	17	18	19	20
N. clusters	5	2|2	1|4	1|1	3|3	1|1	2|2	1|2	1|2	3|1	1|1	1|3	2|2	1|3	1|1	1|1	1|2	2|3	2|3	2|2	1|1
	15	4|4	2|7	1|1	4|7	3|3	4|3	3|2	1|2	3|2	2|2	2|4	3|5	1|5	2|1	2|4	2|4	2|3	1|5	3|2	2|2
	25	5|5	2|10	1|1	7|9	3|3	5|4	3|2	2|2	4|3	5|3	2|5	4|5	2|6	3|1	3|4	2|5	2|4	1|5	2|2	2|3
		4	5	1	5	3	3	2	2	3	3	4	5	5	1	4	4	2	5	2	2

Table 5: Number of unique Swiss spatial clusters representing >90% of gridcells in each modelled region, based on Spectral and k-means clustering applied to all Swiss gridcells (shown in Figure 15) to create 5, 15, and 25 clusters. The 20 numbered columns represent our Swiss modelled regions (see sub-section 2.2, which predominantly match cantonal borders. The last row of the table is our choice of the number of sub-regions per modelled region into which we cluster the turbine capacity factor data.

9 Appendix - Baseline: Swiss energy perspectives 2050+

The Swiss Energy Perspectives 2050+ (EP 2050+)[5] are a set of scenarios for Swiss energy system development that are in line with the Energy Strategy 2050, to reach net-zero emissions by 2050 with a phase-out of nuclear power by 2035. Published in November 2020 **[ref]**, the EP 2050+ are the most up-to-date scenarios describing a net-zero emissions 2050 Swiss energy system developed on behalf of the Swiss Federal Office of Energy (SFOE). The EP 2050+ scenarios

[4] Figure 15 shows our model regions, which are based on cantonal borders. For more information, see sub-section 2.2.

[5] https://www.bfe.admin.ch/bfe/en/home/policy/energy-perspectives-2050-plus.html

are: ZERO basis, ZERO A, ZERO B, and ZERO C. All assume net-zero emissions in Switzerland, with ZERO A-C scenarios being variants of ZERO basis. To reach carbon-neutrality, all EP 2050+ scenarios focus on energy efficiency and renewable energy generation. In the variant scenarios, the only changes made are the degree of reliance on electrification, hydrogen-derived fuels, and biomass-derived fuels to meet heat and transport demands.

In this project, we use only the ZERO basis scenario from the EP 2050+. ZERO basis acts as the baseline from which we generate all our other energy system design alternatives. However, we cannot constrain our system to match ZERO basis exactly, since not all data is available to do so, and our assumptions on the rest of Europe may make the exact ZERO basis system configuration impossible to achieve (the EP 2050+ only explicitly model Switzerland). Instead, we use the scenario's relative reliance on different technologies to meet demands. Hence, one should not expect our results with respect to ZERO basis to match those given by the EP 2050+.

The components of the EP 2050+ ZERO basis scenario that we will use in our baseline run are the following:

- increase in annual Hydropower production (+5%);
- increase in pumped storage discharge capacity (+2.8GW);
- continued electricity agreement between Switzerland and neighbouring countries, with potential for increased cross-border capacities compared to today;
- reduction of final energy consumption for space heating (-31%) and building appliances and cooling (-29%);
- change in waste incineration potential to 2050 (0%); and
- maximum flexible EV charging (50% of EV fleet).

The components of the EP 2050+ ZERO basis scenario that we will not use in our baseline run are the following:

- ability to import biomass. This should not impact the potential contribution of biomass, since our estimate for residual biomass potential (41 TWh) [24] is higher than the ZERO basis modelled consumption, including imports (36 TWh);
- inclusion of geothermal energy. This is deemed to be a minor contributor in the EP 2050+ (<5% of district heat and electricity generation);
- thermal storage capacity of building envelopes. Instead, thermal storage capacity is available only in low-temperature water storage tanks (with an associated investment cost penalty);
- combined PV and battery storage. In the EP 2050+, approximately 70% of PV installations are expected to be coupled with batteries. Rather than assume this, we allow the model to decide on the degree of battery installations in which to invest;

- limit of PV production to building-mounted installations. The EP 2050+ does not consider the possibility of ground-mounted solar photovoltaic (PV) installations (i.e., those on open fields). We allow up to 50% of PV electricity generation to originate from ground-mounted PV installations;
- degree of vehicle and building-level heat electrification. It is not clear from the report exactly how much of final energy demand for mobility and building heat are met by these technologies;
- ratio of PV to wind electricity generation (8:1). Since we generate a broad range of alternatives, and particularly many ways in which wind generation could contribute to the Swiss energy system, these shall naturally include options with varying ratio of PV to wind; we consider all of them, rather than limiting ourselves to only a fixed possibility. In addition, we impose a minimum wind power deployment of 1 GW, to avoid wasting computational power on the generation of system design options without any wind power.
- contribution of district heating to final energy consumption for building heat (25%), share of synthetic fuels imported from abroad (100%), degree of Swiss self-sufficiency (76% domestic production). For all these features, the same considerations made above for the PV-to-wind ratio apply: we generate a broad range of options that shall include many possibilities, influenced by the varying role of wind energy in our option space compared to limited one assumed in the ZERO Basis scenario.